AD-A281 337

MENTATION PAGE

Form Approved
OMB No 0704-0188

2. REPORT DATE	3. REPORT TYPE AND DATES COVERED
26 May 1994	final 1 Feb 91 - 31 Mar 94

4. TITLE AND SUBTITLE
Adaptive Control of Nonlinear Flexible Systems

5. FUNDING NUMBERS
DAAL03-91-C-0011

6. AUTHOR(S)
Dr. Robert L. Kosut
Dr. M. Guntekin Kabuli

7. PERFORMING ORGANIZATION NAME(S) AND ADDRESS(ES)
Integrated Systems Inc.
3260 Jay Street
Santa Clara, CA 95054-3309

8. PERFORMING ORGANIZATION REPORT NUMBER

9. SPONSORING / MONITORING AGENCY NAME(S) AND ADDRESS(ES)
U.S. Army Research Office
P. O. Box 12211
Research Triangle Park, NC 27709-2211

10. SPONSORING / MONITORING AGENCY REPORT NUMBER
ARO 28350.2-EG

11. SUPPLEMENTARY NOTES
The view, opinions and/or findings contained in this report are those of the author(s) and should not be construed as an official Department of the Army position, policy, or decision, unless so designated by other documentation.

12a. DISTRIBUTION / AVAILABILITY STATEMENT
Approved for public release; distribution unlimited.

12b. DISTRIBUTION CODE

13. ABSTRACT *(Maximum 200 words)*

The objective is the development of adaptive control methods which can significantly improve closed-loop performance for a broad class of nonlinear flexible systems. Towards this end, a nonlinear controller, applicable to a broad class of nonlinear systems, was devised. The controller consists of a feedforward signal generator which incorporates a model estimate together with a global feedback linearizer. There is an inner feedback controller which modifies control action in accordance with output errors between the feedforward ideal output and the actual sensed output. The adaptive scheme studied uses measured data to update the model in the feedforward signal generator. It was discovered in many simulations that this two-level approach to adaptive feedback linearization can perform significantly better than feedback linearizers using an observer network.

14. SUBJECT TERMS	15. NUMBER OF PAGES
adaptive nonlinear control, feedback linearization	55
	16. PRICE CODE

17. SECURITY CLASSIFICATION OF REPORT	18. SECURITY CLASSIFICATION OF THIS PAGE	19. SECURITY CLASSIFICATION OF ABSTRACT	20. LIMITATION OF ABSTRACT
UNCLASSIFIED	UNCLASSIFIED	UNCLASSIFIED	UL

integrated systems

Final Report

Contract No: DAAL03-91-C-0011

Adaptive Control of Nonlinear Flexible Systems

Prepared by:

Dr. Robert L. Kosut
Dr. M. Güntekin Kabuli
Integrated Systems Inc.
3260 Jay Street
Santa Clara, California 95054-3309

Prepared for:

US Army Research Office
P.O. Box 12211
Research Triangle Park
North Carolina 27709-2211

ISI Report No. 5923-1

May 26, 1994

Integrated Systems, Inc.
3260 Jay Street
Santa Clara, CA 95054-3309
Tel: 408.980.1500 Fax: 408.980.0400

Contents

1 Introduction **1**

1.1 Research Objectives 1

1.2 Publications 2

1.3 Personnel 3

1.4 Interactions 3

2 Technical Discussion **5**

2.1 Overview 5

2.2 Review of Feedback Linearization 7

2.3 Feedforward System Design 9

2.3.1 Nominal Design 9

2.3.2 Coping with Unstable Zero-dynamics 11

2.3.3 Incorporating Disturbance Models in the Nominal Design 12

2.4 Feedback System Design 15

2.4.1 Time-varying Controller Design 16

2.5 Adaptation 18

2.5.1 Application to Adaptive Testbed 18

2.6 Towards a Nonlinear Control Design Based on Measured Variables 19

2.6.1 Example 1: Tracking and Nonminimum-Phase Zero Dynamics 24

2.6.2 Making the Separation Principle Work 26

2.6.3 Example 2 27

3 References **31**

Appendix A **33**

Appendix B **41**

Appendix C **49**

1 Introduction

Many of the envisioned future Army missions will involve high performance feedback control of uncertain nonlinear systems. For example, control and stabilization of helicopter based weapons platforms, precision gun stabilization and pointing, and the use of lightweight robots for munitions loading all pose difficult nonlinear control problems. In general, nonlinearities in mechanical systems arise from a number of sources, such as, actuator saturation, friction in bearings or gear trains, backlash due to gear spacing or slippage, kinematic transformations, and aerodynamic forces. Additionally, many of these systems are also flexible, with nonlinear damping mechanisms. In many cases the type of nonlinearity as well as their parameter values are not very well known and prior knowledge is too coarse to guarantee acceptable closed-loop performance. Under these conditions, it is necessary to adapt the controller by estimating the uncertain model parameters from on-line data.

1.1 Research Objectives

The objective of this work is the development of adaptive control methods which can significantly improve closed-loop performance for a broad class of nonlinear flexible systems.

Towards this end, the goals were as follows:

1. Form a parametric model representing a broad class of nonlinear flexible systems.
2. Design a nonlinear controller based on the parametric model which provides desired closed-loop performance if the parameters were known.
3. Identify the parameters of the system using measured data and use these estimates in the controller.
4. Analyze the stability and performance properties of the complete adaptive system using the method of averaging.

We concentrated most of our effort on items 1 and 2 as these turned out to be the most difficult and challenging tasks. These must first be resolved in order to proceed to adaptation (items 3 and 4).

In general, the final adaptive system described above fits into the generic adaptive scheme depicted in Figure 1.1.

In this traditional adaptive control system, often referred to as the self-tuning-regulator (STR), [2], the identified model is usually selected out of a model set with unknown parameters. The controller is designed as if the parameter estimates were in fact the correct parameters for describing the plant. In the ideal case it is assumed that there exist parameters, which if known, would precisely account for the measured data. Even in this ideal case, the transient errors between the identified model and the true system can be so large as to completely disrupt performance. In the usual (non-ideal) case – the true system is not in the model set – both unacceptable transient or asymptotic behavior can occur *e.g.*, [1].

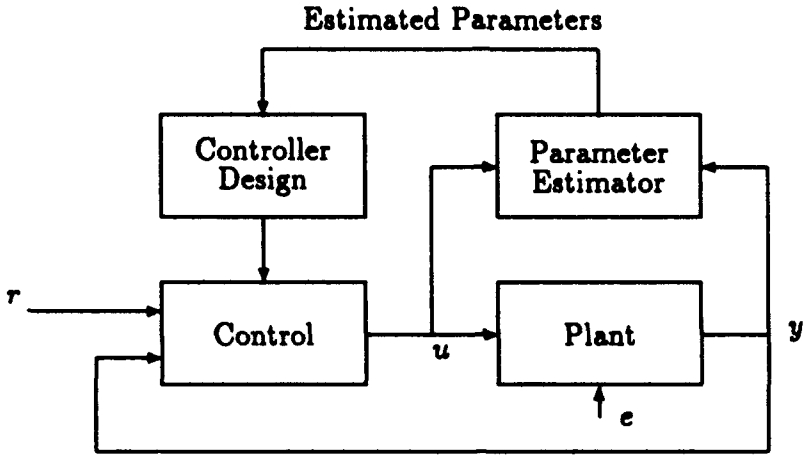

Figure 1.1: Adaptive control system with parameter estimator.

The above cited problems are well documented in the case of adaptive linear control, *i.e.*, when the adaptive parameters are held fixed the closed-loop system is linear. However, the case considered here is adaptive *nonlinear* control, *i.e.*, when the adaptive parameters are held fixed the closed-loop system is nonlinear. Naturally the same problems will arise in this case as in the adaptive linear case. Unfortunately many of the controller design and parameter estimator issues have not been developed sufficiently as yet. In consequence, the first step has been to resolve some of these issues.

1.2 Publications

The following is a list of publications during the reporting period. Items 2,3 and 4 are included as Appendices.

1. "On sensitivity of adaptive feedback linearization: a case study," Robert L. Kosut and M. Güntekin Kabuli, *Proceedings of the 7th Yale Workshop on Adaptive and Learning Systems*,New Haven, Connecticut, May 20–22, 1992.

2. "Adaptive feedback linearization: implementability and robustness," M. Güntekin Kabuli and Robert L. Kosut, *Proceedings of the 31st IEEE Conference on Decision and Control*, pp. 251–256, Tucson, Arizona, December 1992.

3. "On feedback linearizable plants," M. Güntekin Kabuli and Robert L. Kosut, *Proceedings of the American Control Conference*, pp. 1186–1190, San Francisco, June 1993.

4. "Real-time implementation issues in nonlinear model inversion," M. Güntekin Kabuli, Sudarshan P. Bhat and Robert L. Kosut, *Proceedings of the American Control Conference*, pp. 547–551, San Francisco, June 1993.

1.3 Personnel

Dr. Robert Kosut and Dr. M. Güntekin Kabuli worked on the project during the reporting period 1 February 1991 through 30 April 1994.

1.4 Interactions

We have had several interactions with Norm Coleman's group at ARDEC. As a proof-of-concept, the proposed model-follower based feedforward-feedback control design was applied to the analytical model of the Advanced Weapons Testbed at ARDEC, which is a central topic of the ARO Workshops on Real-Time Control. The findings were presented at the 2nd ARO Workshop on Real-Time Control at ARDEC, 17-18 June 1992.

Some of the work reported here was jointly supported by the AFOSR Directorate of Aerospace Sciences, under contract F49620–90–C–0064 .

2 Technical Discussion

2.1 Overview

With few exceptions, practically all of recent research in adaptive control is for the case of *parameter adaptive linear systems*, i.e., when the adaptive parameters are held fixed, the resulting system is linear-time-invariant (LTI), e.g., [1, 2]. In our current effort, we have examined *parameter adaptive nonlinear systems*, that is, when the adaptive parameters are held fixed, the resulting closed-loop system is nonlinear. Although this is an active field of research, (see, e.g. [10, 14]) our efforts to date have convinced us that parameter adaptation *cannot* be introduced unless there is an adequate nonlinear control design. Specifically, *a necessary first step to realizing a practical adaptive nonlinear control is to design a nonlinear control system which is robust to parameter variations.* Because of this, in our most recent efforts we have concentrated exclusively on the design of a (non-adaptive) nonlinear robust control system.

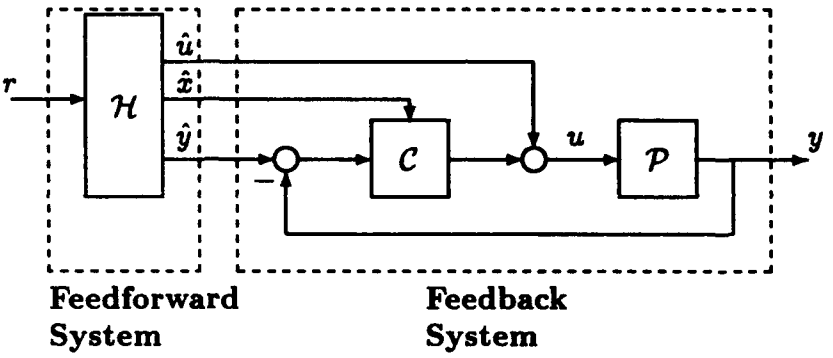

Figure 2.1: Model-follower nonlinear feedback system.

Our current research in this direction has led us to the configuration shown in Figure 2.1, which we refer to as a *model-following feedback system.* We have discovered that this scheme is very well suited for both tracking and regulation of nonlinear systems [7] . In addition, it is easily extensible to parameter adaptation as explained below. The structure in Figure 2.1 is actually quite generic, e.g., the major elements appear in most flight control systems. Such a structure has been successfully used in nonlinear models involving jet engine/propulsion control systems [15] . Many simulation studies as well as preliminary theoretical results show that the configuration has some very nice properties. Specifically :

- The controller design can be conveniently separated into two design steps: (1) design a feedforward signal generator $\mathcal{H}$, and (2) design a feedback regulator $\mathcal{C}$. These steps are not entirely uncoupled and the issues involved are discussed in Section 2.4 .
- The feedforward signal, $\hat{u}$, is designed using an idealization or model of the plant. Hence, the feedforward system signal $\hat{y}$, is the ideal output. The innovative idea for the feedforward design, is to use feedback linearization techniques [5, 10] to design the

map from the reference command r to $\hat{y}$, the ideal output.[1] Hence, the feedforward system *globally and directly* accounts for the plant nonlinearities. No linearization and subsequent elaborate schemes for "scheduling" linear models is required. There are a number of important unresolved issues. For example, input to output feedback linearization based design is limited to minimum phase plants. In addition, a feedforward design based on an ideal model may result in too demanding a control. Hence, by accounting for plant perturbations, the feedforward signal can be made more cautious. Suggestions for resolving these issues are proposed herein.

- The feedback regulator $\mathcal{C}$ is designed to correct for (hopefully) small deviations between the actual sensed output y and the ideal output $\hat{y}$. These deviations are caused by disturbances as well as modeling errors between the actual nonlinear plant $\mathcal{P}$ and the model used to design $\mathcal{H}$ and $\mathcal{C}$. Currently, we have investigated a number of methods for designing $\mathcal{C}$. In particular:

  - Linearization about equilibria results in a collection of LTI designs for $\mathcal{C}$ for which standard gain-scheduling approaches can be used to link the designs. In numerous simulation studies we have noted excellent robust behavior even for a *single* LTI regulator design, e.g., see [8] which is included in Appendix A .
  - We have examined linearization about the model-follower non-equilibrium state, resulting in linear-time-varying (LTV) control design. A specific idea is put forth in (see Section 2.4.1) .
  - The regulator can also be designed as a nonlinear controller whose local properties may be significantly more robust than either the LTI or LTV designs (see Section 2.3.3) .

- Adaptation can take place in either $\mathcal{H}$ and/or $\mathcal{C}$. Adaptation in $\mathcal{H}$ only affects the tracking performance, whereas adaptation in $\mathcal{C}$ affects principally regulation, but also affects tracking.

In summary, the key feature of the proposed scheme in Figure 2.1 is that the controller $\mathcal{H}, \mathcal{C}$ is implementable, i.e., it depends only on the available signals r, y. This is unlike designs based solely on feedback linearization methods which rely on state availability, and hence, are not implementable. The innovation here uses the power of feedback linearization to generate feedforward signals which render harmless the dominant negative effects of the plant nonlinearity. We have also studied parameter adaptation and some of the results are contained in Appendix A . In this case, if the underlying nonlinear control scheme is not robust, then what happens is precisely the same as in the case of parameter adaptive linear systems. The instantaneous plant and estimated model mismatch can induce an unacceptable transient, even if there is asymptotic convergence, e.g., [1, 2] .

[1] A brief review of feedback linearization is provided in Section 2.2

2.2 Review of Feedback Linearization

A major element in our effort is the use of feedback linearization methods for designing $\mathcal{H}$, the feedforward system in Figure 2.1 . To appreciate the issues, and why we chose this configuration, we will first provide a brief review of feedback linearization.

The underlying theory shows that a large class of nonlinear control systems can be made to have linear input-output behaviour by virtue of nonlinear state feedback. In the course of tracking controller design using feedback linearization, the terms *zero-dynamics* and *relative degree* (see e.g., [5] and references therein) are used to describe the limitations of the approach. Loosely speaking, the relative degree is the number of differentiations one has to perform at the output to reach the control input. The zero-dynamics is the dynamics that is rendered unobservable when feedback linearization is performed to obtain an LTI input-output description whose transfer function has the associated relative degree. A nonlinear input-output map that exhibits stable zero dynamics is also referred to as *minimum-phase* . As an illustration, consider the disturbance-free plant system:

$$\begin{aligned} \dot{x} &= Ax + f(x) + Bu \qquad & x \in \mathbb{R}^n \\ y &= Cx & y, u \in \mathbb{R}^m \ , \ m \leq n \quad . \end{aligned}$$

Suppose that CB is invertible, and for simplicity let

$$CB = I \quad .$$

Then,

$$\dot{y} = C(Ax + f(x)) + u \quad .$$

Since u affects all elements of y after one differentiation, the system is said to have *relative degree one* . Moreover, applying the nonlinear state feedback

$$u = v - C(Ax + f(x))$$

renders linear the input-output system from v to y . That is,

$$\dot{y} = v \quad .$$

Choosing

$$v = \Lambda(r - y)$$

gives

$$\dot{y} = \Lambda(r - y) \quad .$$

Hence, if Λ is strictly Hurwitz, then r to y is a stable LTI system.

Note that, in the above process, $n - m$ states are rendered unobservable. Hence, even if y is bounded, the remaining states of the closed-loop system (the zero dynamics) need not be. Thus, feedback linearization is a plant inversion based control design approach, and is stabilizing provided that the associated zero dynamics are stable.

The feedback linearization procedure can be applied to more general disturbance-free systems of the form

$$\begin{aligned} \dot{x} &= f(x) + G(x)u \qquad x \in \mathbb{R}^n \\ y &= h(x) \qquad\qquad\quad y, u \in \mathbb{R}^m \quad . \end{aligned}$$

Under certain conditions involving f and G (*controllability* and *involutivity* [5]), there exists an invertible coordinate transformation

$$\xi = \Phi(x) \ , \ x = \Phi^{-1}(\xi)$$

such that

$$\begin{aligned} \dot{\xi} &= A\xi + B(\alpha(\xi) + \beta(\xi)u) \\ y &= h(\Phi^{-1}(\xi)) \end{aligned}$$

and $\beta(\xi)$ is invertible. Then,

$$u = \beta(\xi)^{-1}[v - \alpha(\xi)]$$

renders linear v to ξ . That is

$$\begin{aligned} \dot{\xi} &= A\xi + Bv \\ y &= h(\Phi^{-1}(\xi)) \quad . \end{aligned}$$

Since the system from v to ξ is now LTI, standard LTI control designs for v are easily accomplished. In addition if Φ can be chosen such that $h(\Phi^{-1}(\xi)) = C\xi$, for some matrix C , then the map from v to y is also LTI. Note that for this case, the LTI system (A, B, C) need not be minimum-phase.

Despite the ease of control design in the transformed coordinates, feedback linearization based approaches have some serious drawbacks:

- control laws are *state* dependent and usually the states are not completely available as sensed variables. Hence, the motivation to use feedback linearization only in $\mathcal{H}$ as in Figure 2.2 .
- the effect of disturbances on the transformations and designed control laws cannot be guaranteed unless certain *matching conditions* hold [5] .
- the nonlinear transformations may not be valid if plant parameters change or are uncertain.
- in the control of flexible systems, plant models are often non-minimum phase.
- even when linear parametric models are used in one state-space description, switching to another state-space description by nonlinear transformations results in multilinear parametric dependencies. Hence, in order to apply adaptation laws for linear parametric models, overparametrization is required, i.e., the number of adapted parameters increases.

Clearly, the power of feedback linearization is in directly handling the system nonlinearities. However, the unavailability of a full-state measurement hinders the applicability. For this reason, we chose the configuration of Figure 2.1 .

2.3 Feedforward System Design

We use feedback linearization methods in the design of the feedforward system $\mathcal{H}$ (see Figure 2.2) , such that:

- the feedforward system $\mathcal{H}$ achieves some desired specifications when disturbances are zero (nominal design) ,
- the feedforward system exhibits satisfactory performance for preset bounded but unknown disturbances (perturbation study of the nominal design) .
- the performance of the nominal design is robust under model variations in a specified model set.

In the above scenario, the disturbances and/or model variations do *not exist in* $\mathcal{H}$, because it is a feedforward signal generator. However, the resulting signal pairs $(\hat{u}, \hat{y})$ can be designed in *anticipation* of such scenarios, thereby reducing the task of the regulator to be robust.

2.3.1 Nominal Design

For the tracking controller design in $\mathcal{H}$ (Figure 2.1) , consider the interconnection in Figure 2.2 . Note that the internal signals associated with the copy of the model is available by construction (e.g., states $\hat{x}$) . For the nominal design part, assume that the disturbances $d_{\hat{x}}$, $d_{\hat{u}}$ and $d_{\hat{y}}$ are all zero.

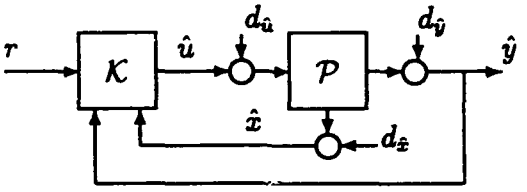

Figure 2.2: Feedforward system

Apart from the issues mentioned in Section 2.2 regarding zero dynamics and coordinate transformations, there are also some inherent limitations due to the nonlinear nature of the control design problem.

Unlike linear systems, nonlinear systems (or operators) are not *right* distributive, i.e., $\mathcal{F}(x+y) \neq \mathcal{F}x + \mathcal{F}y$. The impact of this restriction can be seen by examining the effect of disturbances. Consider a bounded input disturbance d_u and a stable nonlinear $\mathcal{F}$, where

$$y = \mathcal{F}(u + d_u) \quad .$$

The output y can also be expressed as

$$y = \mathcal{F}u + d_y \quad ,$$

where

$$d_y = \mathcal{F}(u + d_u) - \mathcal{F}u \quad .$$

If $\mathcal{F}$ is linear, d_y is also a bounded disturbance, with a bound depending only on the bound of d_u and independent of the input signal u . This property of linear stable maps can be generalized to what is called as incrementally stable nonlinear maps, where bounded deviations about input signals result in bounded deviations at the output signals ; moreover, an output deviation bound can be chosen in terms of the input deviation alone. In other words, the uniform Lipschitz property in the algebraic nonlinearities is extended to include nonlinear dynamic systems. Such an assumption on the subsystems in a feedback system may indeed be quite conservative. We now illustrate the conservatism of imposing Lipschitz conditions in equivalent state-space descriptions.

Typically, the plant model is expressed in terms of states that have physical meaning (e.g., position, rate, etc.) . In the process of control design using feedback linearization, nonlinear coordinate transformations are used to obtain a state-space description where the control is easier to express. Such transformations can drastically change the nature of the nonlinearities in different state-space descriptions. As an illustrative example, consider the map $\mathcal{P}$ from u to y described by

$$\begin{aligned} \dot{x}_1 &= x_2 + f(x_1) \\ \dot{x}_2 &= x_3 \\ \dot{x}_3 &= u \\ y &= x_1 \quad , \end{aligned}$$

where the algebraic nonlinearity f is Lipschitz, i.e., there *exists* a $k > 0$ *such that* $|f(x+y) - f(x)| \leq k|y|$, for all x and y in $\mathbb{R}$. Provided that f is at least twice differentiable, consider the coordinate transformation from x to ξ, where

$$\xi = \begin{bmatrix} x_1 \\ x_2 + f(x_1) \\ x_3 + x_2 f^{(1)}(x_1) + f(x_1) f^{(1)}(x_1) \end{bmatrix}$$

In terms of the state-ξ , the same input-output map can be expressed as

$$\begin{aligned} \dot{\xi}_1 &= \xi_2 \\ \dot{\xi}_2 &= \xi_3 \\ \dot{\xi}_3 &= u + \xi_3 f^{(1)}(\xi_1) + \xi_2^2 f^{(2)}(\xi_1) \\ y &= \xi_1 \quad . \end{aligned}$$

Clearly, unless $f^{(2)}$ vanishes, the nonlinearities in the ξ coordinates will not be Lipschitz . Hence, when determining a stabilizing law of the form

$$u = v - \xi_3 f^{(1)}(\xi_1) - \xi_2^2 f^{(2)}(\xi_1) \quad ,$$

the choice of v can make a considerable difference when a bounded perturbation of ξ_2 is used instead of ξ_2 (see Section 2.3.3) .

With these generic limitations at hand, the following subsections propose methods to cope with unstable zero-dynamics and design stabilizing control laws subject to bounded disturbances. Again, all the proposed controllers are *state dependent* which is permissible only in the design of $\mathcal{H}$, the feedforward signal generator.

2.3.2 Coping with Unstable Zero-dynamics

As mentioned before, a design technique based on plant inversion will be stabilizing provided that the zero dynamics are stable. When the zero-dynamics is not stable, regardless of the relative degree, a control law based on plant inversion cannot be designed. There are two possible ways to avoid explicit plant inversion:

- Construct an output different from the original output with a relative degree of one and with stable zero-dynamics. Hence, asymptotic tracking of the original output can be achieved through the control of this constructed output. Promising results based on this two step procedure have been reported in aerospace applications where unstable zero-dynamics are associated with the acceleration outputs. Feedback linearization was successfully applied to the control of wind angle components (angle-of-attack and sideslip angle). Normal and lateral accelerations were then controlled via integral feedback built upon the wind-angle controller [16, 17] .
- For certain classes of input-output maps with unstable zero dynamics, a nonlinear tracking controller can be designed without going through transformations involving higher order derivatives. In the following, we describe two such classes. These methods can be considered as *approximate* plant inversion.

Consider the class of plants as shown in Figure 2.3 . In this case, the nonlinear system from u to y can be decomposed as

$$\mathcal{P} = P_2 \mathcal{P}_1 \quad ,$$

where $\mathcal{P}_1$ is a nonlinear system but has *minimum*-phase zero dynamics. The map P_2 from z to y is an LTI map with unstable transmission zeros. Hence, the zeros of P_2 are the source of the unstable zero dynamics.

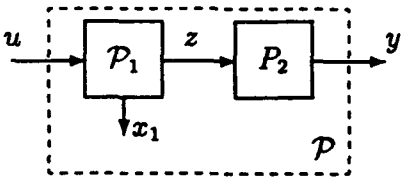

Figure 2.3:

By applying standard input-output linearization to $\mathcal{P}_1$ in terms of z and its state x_1 , a control v can be constructed such that the map from v to z is LTI and stable (recall that in the feedforward system design, all signals are available by construction) . Denote this stable transfer function by H_{zv} . Now the tracking problem reduces to that of designing a tracking controller for the *linear* system from v to y (not necessarily stable), where

$$y = P_2 H_{zv} v \quad .$$

Clearly, this LTI problem is easy to solve.

As a second example, consider the nonlinear system $\mathcal{P}$ shown in Figure 2.4 , where the subsystem P_1 is LTI but possibly unstable and nonminimum-phase. The subsystem $\mathcal{P}_2$ is nonlinear and stable (not necessarily algebraic) .

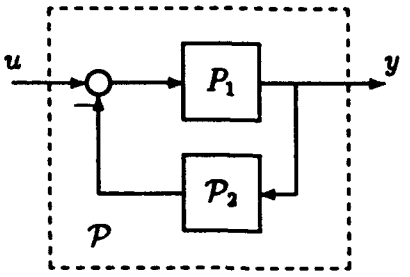

Figure 2.4:

For the interconnection in Figure 2.4 , since $\mathcal{P}_2$ is stable, the zero dynamics is completely determined by that of the LTI subsystem zeros. Due to perfect information in the feedforward system, the control

$$u = \mathcal{P}_2 y + C(r - y) \quad ,$$

renders the map from r to y LTI, for any LTI C that stabilizes P_1 in the unity-feedback configuration.

2.3.3 Incorporating Disturbance Models in the Nominal Design

Once a nominal design is obtained for the disturbance-free case, the interconnection in Figure 2.2 is guaranteed to be only locally stable. From an analysis point of view, such local results may be satisfactory. However, when the goal is control design, subject to a preset bounded but unknown disturbance, the design procedure must be suitably modified. In fact, it may be necessary to resort to nonlinear control design in the transformed coordinates as well.

The following points emphasize some of the reasons why the feedforward system design is posed as in Figure 2.2 :

- The feedforward system is in fact a benchmark design, since its performance is that of the ideal case where the inner-loop controller is operating on zero errors.

- During the implementation of the controller, errors will be introduced in subsystem computations; hence necessarily, the feedforward system performance should be guaranteed for disturbances as shown in Figure 2.2 .

- By guaranteeing a stable system in Figure 2.2 that exhibits desired properties for the class of disturbances under consideration, one can construct a *family* of input-output pairs $(\hat{u}, \hat{y})$, consistent with the model, rather than a single one. Such a capability establishes the first steps towards robustness under model uncertainty.

In the following, we emphasize the need for nonlinear control in the transformed coordinates when the design has to accommodate possibly persistently exciting bounded disturbances. First, the class of plants is described with motivating cases that lead to the associated structure. Second, the approach is described and illustrated by an example. Finally, the extension of the particular approach to incorporate time-variations in the plant as well as the feedback law is discussed.

Consider the stabilization of a perturbed controllable canonical form description:

$$\begin{aligned} \dot{\xi} &= A\xi + B[\alpha(\xi + d_1) + \beta(\xi + d_2)(u + d_3)] + d_4 \\ y &= \xi \end{aligned}$$

with (A, B) a controllable pair, ξ available, but the disturbance d unknown, except that it is bounded with a known bound, independent of ξ . As emphasized before, even if the nonlinearities in the original states is Lipschitz, the transformed state-descriptions will almost always have non-Lipschitz nonlinearities. This problem will arise when

1. the states are available, but there are measurement and actuation disturbances during implementation, or

2. there is a state-ξ estimator which supplies an estimate $\hat{\xi}$ with up to first order bounded state estimation error. Although the separation principle does not hold in general for nonlinear systems, such an estimator can be used in a robust state-feedback (hence, a coupled design) to yield implementable stabilizing controllers.

In the following, $\|\cdot\|$ will denote the sup norm on signals, thus allowing persistently exciting finite average power signals. In the above setup, ξ will be available; however, $d = [d_1^T \; d_2^T \; d_3 \; d_4^T]^T$ is not known, except that $\|d\| \leq \gamma$, for some positive known γ . This particular plant description is motivated by the controllable canonical form within the context of feedback linerizable plants [5] , i.e.:

$$\dot{x} = Ax + B[\alpha(x) + \beta(x)u] \quad ,$$

where (A, B) is a controllable pair; the algebraic functions α and β denote the transformed nonlinear system, β is nonsingular for $x \in \mathbb{R}^n$. When state-x is available, the control law $u = \frac{1}{\beta(x)}(-Kx - \alpha(x))$ steers any initial condition in $\mathbb{R}^n$ to zero asymptotically, provided $(A - BK)$ is strictly Hurwitz. However, such a control law will not be robustly stabilizing when the closed-loop system is subject to unknown but bounded additive disturbances (unless the extremely restrictive case where α and β are Lipschitz) . In order to account for the bounded disturbances, the above feedback linearization based control law needs to be significantly modified.

Approach

To illustrate the approach, consider a single input system in the model set described above (the following ideas can be extended to a multi-input version with a diagonal structure assumption on the function β) .

Due to controllability on $\mathbb{R}^n$, $\beta(\xi) \neq 0$ for any ξ . Apply the control

$$u = -\beta^{-1}(\xi)(\alpha(\xi) + K\xi) + v$$

where K is chosen such that $(A - BK)$ is strictly Hurwitz ; v is to be determined. In fact, in the above control law decomposition, α can be replaced with any function $\hat{\alpha}$ provided that

$$\|(\hat{\alpha} - \alpha)(\xi)\| \leq \gamma_1$$

for all ξ ; i.e., $\hat{\alpha}$ is in a γ_1 tube about the function α . Rearranging terms, one obtains

$$\dot{\xi} \;=\; (A - BK)\xi + d_4 + B\beta(\xi + d_2)(\Delta(\xi, d) + v)$$

where d is unknown but Δ is a known function determined in terms of α , β , d and K . Let ϕ_Δ be such that

$$-\phi_\Delta(\|\xi\|, \gamma) \;\leq\; \Delta(\xi, d) \;\leq\; \phi_\Delta(\|\xi\|, \gamma) \;\;,$$

for all ξ and unknown d . Note that such a bounding function ϕ_Δ can be easily constructed from the known Δ and the bound γ . Recall also that the sign of β is ξ independent. Now choose the term v in the control as

$$v \;=\; -\mathrm{sgn}\beta(0)\mathrm{sgn}(\xi^T \bar{P} B)\phi_\Delta(\|\xi\|, \gamma) \quad ,$$

where the Lyapunov matrix $\bar{P}$ satisfies

$$(A - BK)^T \bar{P} + \bar{P}(A - BK) + Q = 0$$

for some symmetric positive definite Q .

Consider the Lyapunov function candidate $V = \xi^T \bar{P} \xi$; for the above control law, one obtains

$$\dot{V} \;\leq\; -\xi^T Q \xi + 2\xi^T \bar{P} d_4 \quad .$$

The simplified upper bound on $\dot{V}$ is due to the fact that the choice of v renders

$$\xi^T \bar{P} B \beta(\xi + d_2)(\Delta(\xi, d) + v) \;\leq\; 0 \quad ,$$

for all ξ and unknown d . Hence, the nonlinear damping terms in v compensate for the nonlinearity mismatches. It is interesting to note that at any time instant, the cost $V(\xi)$ is not greater than $V(\eta)$, where

$$\dot{\eta} \;=\; (A - BK)\eta + d_4 \quad ,$$

provided that $\xi(0) = \eta(0)$.

Example

Consider the single-input single-output plant

$$\dot{y} \;=\; u \;+\; (y + d_1)^2 \;+\; d_2$$

where y is supposed to track a step reference input r subject to unknown disturbances d_1 and d_2 . Apply the control

$$u = -y^2 - (y - r) + v \quad .$$

Clearly, without the v term to be determined, u is not stabilizing unless $d_1 = 0$; any nonzero mismatch will cause a finite-escape time. Now choose

$$v \;=\; -\delta \mathrm{sgn}(y - r)(\alpha_1 + \alpha_2 |y|) \quad ,$$

where

$$\begin{aligned} |d_1^2 + d_2| &\leq \alpha_1 \\ 2|d_1| &\leq \alpha_2 \end{aligned}$$

The results guarantee asymptotic tracking for $\delta \geq 1$.

Remarks

The above approach is a semi-global stabilization based design; first determine a worst-case bound on the disturbances, and then a design is guaranteed for the specified bounds.

The approach is not limited to the particular model set; in fact, it can be modified to include terms of the form $\alpha(t, \xi, \theta, d)$ where the time-variation and parametric dependence to θ are no longer lumped all in one disturbance term d . Hence, the approach can be made less conservative by e.g., choosing a time-varying bounding function of the form $\phi_\Delta(t, |\xi(t)|, |\theta(t)|, \gamma)$. Clearly, tighter upper bounds will yield less demand on the actuator.

2.4 Feedback System Design

We investigated the following methods:

- designing $\mathcal{C}$ based on linearization about equilibria, thereby resulting in an LTI controller .
- designing $\mathcal{C}$ based on linearization about the ideal trajectories $\hat{u}$, $\hat{y}$, $\hat{x}$ from $\mathcal{H}$. This will result in an LTV controller (see Section 2.4.1) .
- designing $\mathcal{C}$ based on a Lyapunov approach. This will result in a nonlinear controller (see Section 2.3.3) .

Note that all of these methods can be used in the design of $\mathcal{H}$ as well. But the full-state methods used to design $\mathcal{H}$ cannot be used to design $\mathcal{C}$. It is important to emphasize that *all* the signals in $\mathcal{H}$ are *constructed* , whereas $\mathcal{C}$ must be only constructed on *sensed* variables. Thus, the state of $\mathcal{P}$ is *not* available to design $\mathcal{C}$. But the states of a *model* of $\mathcal{P}$ are available to design $\mathcal{H}$ (and also $\mathcal{C}$) .

One of the advantages of the proposed feedback linearization based design of the feedforward system is that the scheduling signal $\hat{x}$ is completely known. It is *constructed* , on line, in $\mathcal{H}$, the feedforward system (see Figure 2.2) .

As an illustration, consider a nonlinear system of the form

$$\begin{aligned} \dot{x} &= f(x) + Bu \\ y &= Cx \quad , \end{aligned}$$

where $f(\cdot)$ is a nonlinear algebraic function and B and C are constant matrices. Following the approaches in Section 2.3 , suppose that the associated tracking problem is solved. In other words, the feedforward system in Figure 2.1 is designed so that

$$\begin{aligned} \dot{\hat{x}} &= f(\hat{x}) + B\hat{u} \\ \hat{y} &= C\hat{x} \end{aligned}$$

where $\hat{y}$ exhibits the desired tracking properties. Note that, all of the variables associated with the feedforward system (i.e., the $\hat{}$ versions) are available by construction.

Now consider a first order approximation to the error system described in terms of $e_x = x - \hat{x}$, $e_y = y - \hat{y}$ and $e_u = u - \hat{u}$. The resulting linear time-varying system can be expressed as

$$\begin{aligned} \dot{e}_x &= A(\hat{x})e_x + Be_u \\ e_y &= Ce_x \end{aligned}$$

where $A(\hat{x}) = \frac{\partial f}{\partial x}(\hat{x})$ is the Jacobian of f evaluated at $\hat{x}$. Because $\hat{x}$ is constructed in the feedforward block $\mathcal{H}$, $A(\hat{x})$ is a ***known*** time-varying matrix. By construction $\hat{x}$ is bounded. Typically, $\hat{x}$ will have the decomposition

$$\hat{x} = \hat{x}_{tr} + \hat{x}_{ss}$$

where $\hat{x}_{tr}$ and $\hat{x}_{ss}$ denote the transient and steady-state components. If the steady-state component is constant, one can design an LTI controller for the equilibrium LTI description. If the steady-state component is periodic and slowly-varying, averaging can be applied to design time-invariant controllers. In the following section, we propose a time-varying controller design approach.

2.4.1 Time-varying Controller Design

Consider the unity-feedback configuration in Figure 2.5 . In the rest of this section we will focus on the case where P is linear-time varying (LTV) . An LTV controller C will be designed so that the closed-loop is stable. Moreover, the controller can be modified (adapted) online to improve the nominal performance.

Suppose that there exists an LTI controller C_0 that stabilizes the unknown LTV plant P . Using stable factor factorizations [18] , let C_0

$$C_0 = ND^{-1} = \widetilde{D}^{-1}\widetilde{N}$$

with the associated Bezout identity

$$\begin{bmatrix} \tilde{U} & \tilde{V} \\ -\widetilde{D} & \widetilde{N} \end{bmatrix} \begin{bmatrix} N & -V \\ D & U \end{bmatrix} = I \quad ,$$

where all of the eight maps are LTI and stable. Under these conditions, all LTV plants that are stabilized by C_0 admit a special factorization:

$$\begin{aligned} P &= \widetilde{D}_p^{-1}\widetilde{N}_p \\ \widetilde{D}_p &= \tilde{V} - Q_p\widetilde{N} \\ \widetilde{N}_p &= \tilde{U} + Q_p\widetilde{D} \quad , \end{aligned}$$

where Q_p is an unknown but stable LTV system. Now, choose an LTV controller $C = N_c D_c^{-1}$, where

$$\begin{aligned} u - \hat{u} &= N_c\xi = (N + VQ_c)\xi \\ \hat{y} - y &= D_c\xi = (D - UQ_c)\xi \end{aligned}$$

Q_c is an LTV stable map to be chosen, and ξ is an available signal by construction of C .

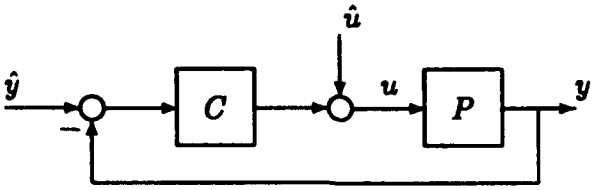

Figure 2.5:

Now, for the specified C and P , the system in Figure 2.5 is stable if and only if the closed-loop map from $(\hat{u}, \hat{y})$ to ξ is stable. Equivalently,

$$\widetilde{D}_p D_c + \widetilde{N}_p N_c = I + Q_p Q_c$$

has a stable inverse. Now suppose that the unknown Q_p has a known gain bound (e.g., an L_2-gain) denoted by $\|Q_p\| < \gamma$. Choose k LTI stable Q_{ci}'s such that,

$$\begin{aligned} \|Q_{ci}\| &\leq 1 \\ \sum_{i=1}^{k} \lambda_i &\leq 1/\gamma \\ Q_c &= \sum_{i=1}^{k} \lambda_i Q_{ci} \quad . \end{aligned}$$

By construction, the gain of $Q_p Q_c$ is less than unity. Hence, by the small gain theorem, $(I + Q_p Q_c)$ has a stable inverse. In other words, for any choice of λ that satisfies the inequality constraint above, the resulting controller will stabilize the unknown P .

The unity-feedback system interconnection also constrains the set of admissible λ values. Writing the summing node equations in Figure 2.5 , we obtain

$$(V\hat{y} - U\hat{u} - \xi) = Q_p(\widetilde{N}\hat{y} + \widetilde{D}\hat{u} + Q_c\xi) \quad .$$

Note that, the above consistency equation is of the form $\eta_1 = Q_p \eta_2$, where η is known, Q_p is unknown but a bound on its gain is available. In the case of predetermined L_2-gain bound on Q_p , the consistency equation translates into inequality constraints on truncated norms of η [13] . Since the controller parameter Q_c is linear in λ , this in turn translates into a quadratic constraint on λ . This quadratic constraint, together with the constraint $\sum_{i=1}^{k} \lambda_i \leq 1/\gamma$ ensure that the choice of λ realizes a stabilizing controller and is consistent with the interconnection equations. Now an additional performance criterion, e.g., the tracking error $D_c\xi$ can be monitored for improvement (the tracking error $D_c\xi$ is affine in the parameter λ) .

2.5 Adaptation

Consider the generic nonlinear plant model shown in Figure 2.6 , where G denotes the ***known*** linear part and $\mathcal{F}$ denotes the algebraic nonlinearity (e.g., friction, saturation) which depends on an ***unknown*** parameter θ . The signals z and v at the input and output of the nonlinearity are ***unavailable*** as measurements. However, for the design of $\mathcal{H}$ in Figure 2.1 , all signals will be available by construction, except that θ will be replaced by the estimate $\hat{\theta}$.

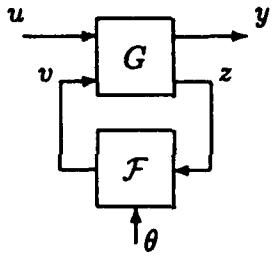

Figure 2.6: A parametric nonlinear plant model $\mathcal{P} : (u, \theta) \mapsto y$.

Once the design of $\mathcal{H}$ is based on $\hat{\theta}$, the interconnection in Figure 2.1 can be modified to that shown in Figure 2.7 . The motivation behind the closed-loop system in Figure 2.7 is that for sufficiently slow adaptation, the performance of the inherent model follower tracking design will be recovered (e.g., [1]) .

2.5.1 Application to Adaptive Testbed

The Adaptive Testbed apparatus at ARDEC poses a particularly interesting nonlinear control design problem suitable for the cascade implementation in Figure 2.1, where:

1. the states are not available as measurements,
2. the model exhibits non-minimum phase zero dynamics
3. the goal is tracking performance improvement
4. an analytical model is available as in Figure 2.6 ,

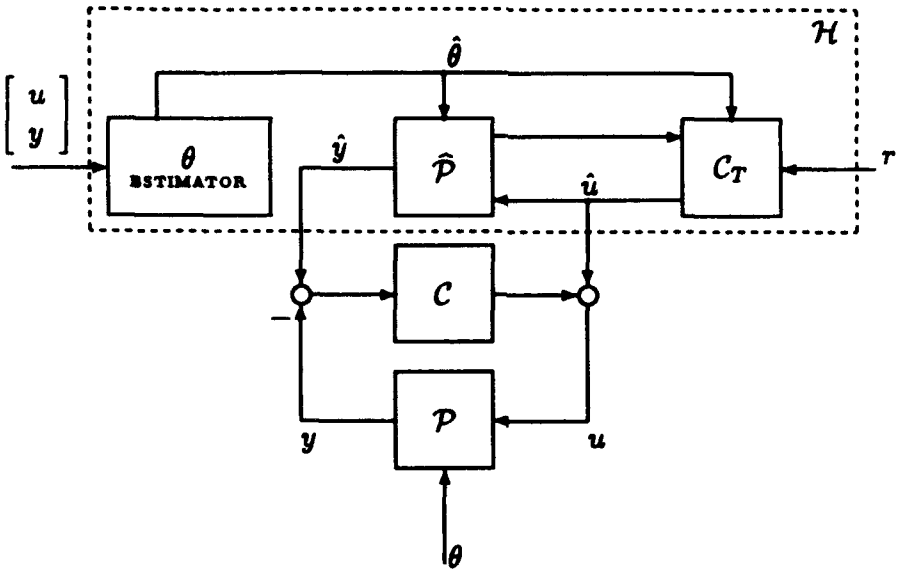

Figure 2.7: Adaptation of the cascade system in Figure 2.1

5. candidate designs can be easily tested out in real-time.

Except for the discrete-controller implementation stage, all of these points coincide with the issues addressed in this research. For the preliminary studies on the analytical model of the testbed, see Appendix C .

2.6 Towards a Nonlinear Control Design Based on Measured Variables

Within the context of finite-dimensional linear time-invariant (LTI) feedback interconnections and LTI plants, full-order estimated state-feedback based design approaches are widely used in control design problems. After suitable augmentations, the design problem is reduced to the stabilization of $\begin{bmatrix} A & B \\ C & 0 \end{bmatrix}$ (can be taken as strictly proper, without any loss of generality) subject to a particular cost criterion (e.g., $\mathcal{H}_2$ and/or $\mathcal{H}_\infty$). The analytical and/or numerical solutions to the associated optimization problem yields a state-feedback gain K and an output-injection gain L , where the matrices $(A-BK)$ and $(A-LC)$ are both strictly Hurwitz. The resulting controller is given by $\begin{bmatrix} A-BK-LC & L \\ -K & 0 \end{bmatrix}$. The relative ease of solutions associated with such design problems stems from the inherent decomposition into two sub-problems which can be dealt with separately. The estimation of the state and the control law based on the ideal state are solved separately, and then the estimated state is used instead of the true plant states in the control law. This two-step approach is referred to as the separation principle.

Before proceeding with nonlinear control design methods and why the separation principle

fails in general, it is useful to observe the inherent properties that make the separation principle work in the LTI setting. Consider the plant $P : u \mapsto y$,

$$\begin{aligned} \dot{x} &= Ax + Bu \\ y &= Cx \end{aligned}$$

with a stabilizable pair (A, B) and a detectable pair (C, A) . If the plant state x were available, a control of the form $u = -Kx$ would solve the stabilization problem. Since x is not available, an estimate $\hat{x}$ is constructed using (u, y) or perturbed versions thereof. Consider the estimator $E : (u_e, y_e) \mapsto \hat{x}$,

$$\dot{\hat{x}} = (A - LC)\hat{x} + Bu_e + Ly_e \quad ,$$

where

$$\begin{aligned} u_e + d_u &= u \\ y + d_y &= y_e \end{aligned}$$

where the exogenous inputs d_u and d_y denote the unmeasured but bounded actuator and sensor disturbances, respectively. Letting $e_x := x - \hat{x}$, and using the estimates in the control, i.e., $u_e = -K\hat{x}$, the closed-loop system is described by

$$\begin{aligned} \dot{x} &= (A - BK)x + BKe_x + Bd_u \\ \dot{e_x} &= (A - LC)e_x + Bd_u - Ld_y \quad . \end{aligned}$$

The properties that make the separation principle work, can be listed as follows:

1. For bounded (d_u, d_y) , e_x is bounded. When $(d_u, d_y) = 0$, $e_x \to 0$.
2. For bounded estimation error e_x , x is bounded. As $e_x \to 0$, $x \to 0$.

Due to possibly persistently exciting disturbance (d_u, d_y) ; e_x is not expected to go to zero. Hence, the state-feedback (in terms of x) must be *robust* to perturbations e_x which does not necessarily correspond to initial conditions mismatches in P and E .

For the sake of argument, suppose that one indeed has an asymptotic observer and a "globally" asymptotically stabilizing full-state feedback law. Intuitively, for "small" errors in the state-estimate, the separation principle based control design will be stabilizing. Thus, after waiting "sufficiently long" for reliably reconstructing the states, one can use the estimated states instead of the true states in the control. Apart from the nontrivial assumption that such an asymptotic observer is available, another pitfall in such an argument is that one may not be able to wait without a nominal bounded-input bounded-output (BIBO)-stabilizing loop, since the plant may blow up before estimation errors are sufficiently small. (e.g., $\dot{x} = x^2 + u$, $u = 0$, $x(0) = x_0 > 0$, $x(t) = \frac{x_0}{1 - tx_0}$) . The existence of such a nominal stabilizing loop is the same as requiring a control that robustly BIBO-stabilizes the plant, although the desired performance may not be achieved.

Imposing the algebraic nonlinearities in the ordinary differential equations to be globally Lipschitz in order to extend the appealing properties of linear vector fields, may be quite

restrictive. Nonlinearities in one coordinate system may be Lipschitz, whereas in an another coordinate system they may not be (recall the discussion on page 10) .

For a given nonlinear plant $\mathcal{P} : u \mapsto y$, consider the tracking problem: for a particular class of reference signals r , determine a control

$$u = \mathcal{K}(r, y)$$

such that $y \to r$ and for a reasonable class of bounded disturbances, under the perturbed control

$$u = d_u + \mathcal{K}(r, y + d_y)$$

the closed-loop signals remain bounded. In other words, the closed-loop (see Figure 2.8) is BIBO-stable (in the sense of a particular extended space) and achieves the desired tracking when disturbances are zero.

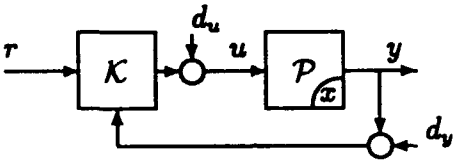

Figure 2.8: Desired dynamic controller $\mathcal{K}$

We will focus on a particular class of single-input nonlinear plants which admit a finite-dimensional state-space description of the form

$$\dot{x} = f(x) + g(x)u$$

for which the State-Space Exact Linearization Problem [5] is solvable over $\mathbb{R}^n$, i.e., controllability and involutivity conditions hold in $\mathbb{R}^n$. For such plants, when states are available, the origin can be rendered globally asymptotically stable. Moreover, when x is available for feedback, the asymptotic tracking problem can be solved for any output that does not introduce a nonminimum-phase zero dynamics. In the case where the output y to track r does introduce a nonminimum-phase zero dynamics, one may be required to introduce dynamic augmentation prior to full-state feedback. Such strong global results do rely on perfect state measurement and render controller candidates as shown in Figure 2.9 .

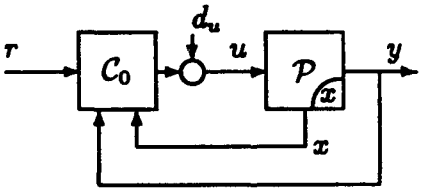

Figure 2.9: Solvable design problem, dynamic controller C_0; $d_x = 0$, $d_y = 0$

Taking into account the control law in Figure 2.8 and the fact that one typically encounters number of sensors much less than the number of states, one might dismiss the plant state based control laws on the grounds that they are not implementable. As it is motivated

by the separation principle based control design, for classes of plants that admit asymptotic observers or in the case of bounded state-estimation errors, the stability properties of the control law with $y = x$ in Figure 2.8 is of major importance (see also Figure 2.11).

Motivated by the separation principle based control design, a design approach can be taken as follows:

- **Assumption :** Imposing stability properties on (u, y) is equivalent to imposing them on x . The plant $\mathcal{P} : u \mapsto y$ does not have any "hidden modes". The input output pair (u, y) completely characterizes the internal dynamics.

- **Problem I :** An estimator that allows the decoupling of the design problem (see Figure 2.10). Recall from the motivating LTI setting, that the role of the estimator is to guarantee that for all bounded d_u, bounded d_y and possibly unbounded u_e , the error $(x - \hat{x})$ is bounded. Moreover, when $d_u = 0$ and $d_y = 0$, $e_x \to 0$. In other words, for the interconnection in Figure 2.10 , the error e_x must be uncontrollable from u and the bound on e_x must depend only on the bound on the exogenous variable d_y . This property is the crux of the separation principle, since it simplifies the design problem to Problem II .

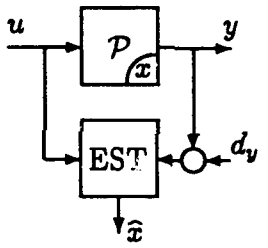

Figure 2.10: Problem I; estimator with $(x - \hat{x}) \in L_\infty$ for all u in $L_{\infty,e}$ and d_y in L_∞

- **Problem II :** A stabilizing state-feedback law. For bounded d_x, d_u and d_y, determine a controller C_1 for which the closed-loop signals remain bounded. Moreover, when $d_u = 0$ and $d_y = 0$, as $d_x \to 0$, $y \to r$. Note that this step is nontrivial since the controller C_0 in Figure 2.9 is typically based on $d_x = 0$ and $d_y = 0$. The local stability properties of the design in Figure 2.9 may not suffice for the specified bound on d_x obtained from Problem I. With a slight abuse of notation, from now on we will refer to C_1 in Figure 2.11 as a robust controller, since its design does take into account the predetermined bounds on d_x and d_y . The abuse is due to the fact that in the LTI setting, robustness is attributed to closed-loop signal dependent perturbations, since exogenous additive disturbances cannot drive a stable LTI loop unstable. Since local and global stability results merge in the LTI setting and global stability results are too restrictive in the nonlinear setting, perhaps a better suited description for the controller C_1 in Figure 2.11 is *semi-global* ; i.e., for the given bounds on d_u,d_x and d_y the closed-loop signals remain bounded.

- **Merging Solutions to Problems I and II :** Recall that the solution to Problem I guarantees that bounded deviations about possibly unbounded input output pairs of

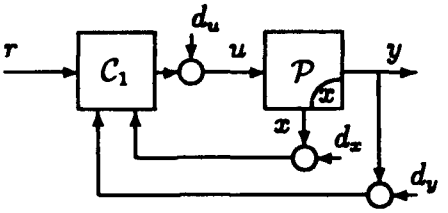

Figure 2.11: Problem II; dynamic controller C_1, possibly different from C_0

$\mathcal{P}$ result in bounded e_x . Hence one can incorporate Figure 2.10 in Figure 2.11 as the bounded disturbance d_x generator to obtain Figure 2.12 .

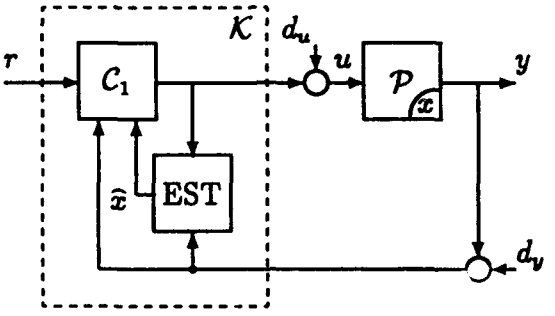

Figure 2.12: Candidate controller $\mathcal{K}$

Note that, in the case that the estimator in Problem I satisfies the property that $e_x \to 0$ for $d_u = 0$ and $d_y = 0$, that is when x is asymptotically reconstructed, the choice of the robust controller C_1 in Problem II guarantees that the closed-loop signals remain bounded due to bounded d_x ; in addition, the nominal design constraint on C_1 ensures that $y \to r$ as $d_x \to 0$.

As a preliminary step towards control design based on state-estimates, the following two studies show the importance of the choice of the nominal globally stabilizing (or tracking) control law based on perfect state measurements.

In the first study, set-point asymptotic tracking problem is solved for an output that exhibits nonminimum-phase zero dynamics. Using dynamic augmentation and then applying state-feedback asymptotic tracking problem is solved. In other words, the controller C_0 in Figure 2.9 is obtained. The derivations emphasize that the standard Lipschitz constraints, for ease of Lyapunov based derivations, on the resulting vector fields after possible changes in coordinates is too restrictive.

In the second study, stability properties of the origin is investigated when the feedback law is based on estimates from an asymptotic observer. It is shown that the globally stabilizing exact feedback linearization based controller C_0 in Figure 2.9 is no longer globally stabilizing in Figure 2.10 . A globally stabilizing controller C_1 that solves the Problem II is constructed. Using the asymptotic observer, the controller $\mathcal{K}$ in Figure 2.12 is obtained.

2.6.1 Example 1: Tracking and Nonminimum-Phase Zero Dynamics

In order to illustrate a strictly causal plant with a one-dimensional possibly nonminimum-phase zero dynamics, consider the following two-state u to y map.

$$\begin{aligned} \dot{x}_1 &= x_2 + f(x_1) \\ \dot{x}_2 &= 4(x_2 - x_1) + u \\ y &= x_2 - x_1 \end{aligned}$$

Note that when $f = 0$, the transfer function from u to y is $\frac{(s-1)}{(s-2)^2}$.

It is easy to see that a tracking control based on the coordinate transformation using derivatives of y will not be stabilizing. Note that

$$\dot{y} = 4y + u - x_2 - f(x_1) \quad .$$

For $\dot{r} = 0$,

$$u = -4y + x_2 + f(x_1) + \alpha(r - y)$$

results in

$$\dot{(y - r)} = -\alpha(y - r) \quad ;$$

hence for any $\alpha > 0$, $y \to r$. However, the asymptotic tracking constraint

$$x_2 = x_1 + y(0)e^{-\alpha t}$$

renders

$$\dot{x}_1 = x_1 + f(x_1) + r + (y(0) - r)e^{-\alpha t} \quad .$$

Take for example, $r = 0$, $f(\cdot) = (\cdot)^3$. Clearly, in the limit

$$\dot{x}_1 = x_1 + x_1^3 \quad ,$$

and the states are unbounded.

When f is zero, it is well known that step inputs can be asymptotically tracked if and only if plant and/or the compensator have at least one pole at zero. Since $\frac{(s-1)}{(s-2)^2}$ does not have a pole at zero, the standard LTI design procedure would involve augmentation with an integrator. Proceed with the same augmentation for the nonlinear plant at hand (see Figure 2.13) .

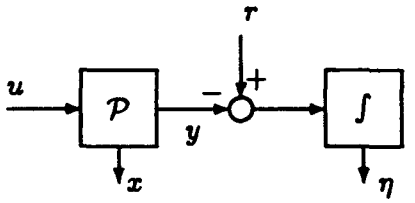

Figure 2.13: Augmented plant

If x were available, since η is part of the controller, the augmented plant states are available. If one can find a relative degree three output, i.e., solve the state-feedback linearization

problem, then $\dot{\eta} \to 0$ would imply that $y \to r$. This requires that the augmented plant dynamics

$$\begin{aligned} \dot{\eta} &= r - x_2 + x_1 \\ \dot{x}_1 &= x_2 + f(x_1) \\ \dot{x}_2 &= 4(x_2 - x_1) + u \end{aligned}$$

satisfies the controllability and involutivity conditions. Both conditions are satisfied provided that

$$f^{(1)}(x_1) \neq -1$$

which we will assume for global results. It is interesting to note that this condition is in fact a generalization to the hidden mode concept in the LTI setting, i.e., if $f(x_1) = -x_1$, the linear plant from u to y would have a hidden unstable mode.

Now consider the relative degree three output

$$z = \eta + x_1$$

motivated by the $f = 0$ case. Note that

$$\begin{aligned} z^{(1)} &= r + x_1 + f(x_1) \\ z^{(2)} &= \underbrace{(1 + f^{(1)}(x_1))}_{\beta(x_1)}(x_2 + f(x_1)) \end{aligned}$$

and recall that the (global) controllability condition is equivalent to $\beta(x_1) \neq 0$ for all $x_1 \in \mathbb{R}$. Hence, under the coordinate transformation

$$\xi = \begin{bmatrix} z \\ z^{(1)} \\ z^{(2)} \end{bmatrix}$$

the augmented plant dynamics can be put into the controllable canonical form

$$\begin{aligned} \dot{\xi}_1 &= \xi_2 \\ \dot{\xi}_2 &= \xi_3 \\ \dot{\xi}_3 &= \underbrace{f^{(2)} \cdot (x_2 + f)^2 + \beta(x_1)(u + 4(x_2 - x_1) + f^{(1)} \cdot (x_2 + f))}_{\alpha(x) + \beta(x_1)u} \end{aligned}$$

where dependencies on x_1 are suppressed in the f terms, for the sake of brevity. For any ψ_1, ψ_2 and ψ_3 such that the polynomial

$$s^3 + \psi_1 s^2 + \psi_2 s + \psi_3$$

is strictly Hurwitz, the control u determined by

$$\alpha(x) + \beta(x_1)u = \psi_3 \xi_1 - \psi_2 \xi_2 - \psi_1 \xi_3$$

renders $\xi = 0$ globally asymptotically stable (recall that the transformation to ξ coordinates is one-to-one and onto) . Hence

$$\begin{aligned} 0 &= r + x_1 + f(x_1) \\ 0 &= \beta(x_1)(x_2 + f(x_1)) \end{aligned}$$

and $\beta(x_1) \neq 0$ imply that

$$r + x_1 - x_2 \to 0$$

i.e., $y \to r$. Note that the above exact cancellation based scheme is not the only way to stabilize the augmented plant in the ξ coordinates. In fact, as we will see later on, such an exact cancellation may make the global nature of the nominal result not robust, i.e., perturbations in the states (other than initial conditions) may render the result only locally stable. Hence, it is crucial that one studies the sensitivity of the full-state based control design and modify it if possible so that for the class of anticipated disturbances, the local nature of the control law is satisfactory.

2.6.2 Making the Separation Principle Work

Consider the plant

$$\begin{aligned} \dot{x} &= Ax + Bu + F(y) \\ y &= Cx \end{aligned}$$

with (A, B, C) a minimal triple. Suppose that there exists a nonlinear coordinate transformation

$$\xi = \Phi(x)$$

such that the plant can be equivalently represented as

$$\begin{aligned} \dot{\xi} &= A\xi + B(u + \alpha(\xi)) \\ y &= C\Phi^{-1}(\xi) \end{aligned}$$

For such a system, asymptotic state construction is easier in the x-coordinates, since

$$\begin{aligned} \dot{\hat{x}} &= A\hat{x} + Bu + F(y) + L(y - \hat{y}) \\ \hat{y} &= C\hat{x} \end{aligned}$$

yields an estimation error $e_x := x - \hat{x}$, where

$$\dot{e_x} = (A - LC)e_x \quad .$$

The stabilizing control is easier to express in the ξ-coordinates since

$$u = -K\xi - \alpha(\xi)$$

renders $\xi = 0$ globally asymptotically stable since the above control yields

$$\dot{\xi} = (A - BK)\xi \quad .$$

The heuristic step of replacing ξ by $\Phi(\hat{x})$ can only guarantee *local* results. For "sufficiently" small e_x , the estimated-state feedback will be locally stabilizing. The crucial points are how large the basin-of-attraction is and if it is possible to enlarge it to yield a satisfactory design.

Let $\hat{\xi} := \Phi(\hat{x})$. The closed-loop dynamics under the feedback law

$$u = -K\hat{\xi} - \alpha(\xi)$$

can be expressed as

$$\dot{\hat{\xi}} = (A - BK)\hat{\xi} + \underbrace{\left.\frac{\partial \Phi}{\partial \hat{x}}\right|_{\hat{x}=\Phi^{-1}(\hat{\xi})}}_{M(\hat{\xi})} \underbrace{\left(LCe_x + F(C\Phi^{-1}(\hat{\xi}) + e_x)) - F(C\Phi^{-1}(\hat{\xi}))\right)}_{G(\hat{\xi}, e_x)}$$

$$\dot{e_x} = (A - LC)e_x$$

Even if F is Lipschitz (hence $\|G(\hat{\xi}, e_x)\|$ depends only on $\|e_x\|$), $M(\hat{\xi})$ need not be Lipschitz. Hence establishing and modifying the basin-of-attraction are nontrivial design tasks. However, the crucial observation is that the stabilization problem is in fact the robustness of the full-state feedback law subject to L_2 disturbances.

The following example illustrates the need for a robust state-feedback law and the sensitivity of the exact-linearization based control law.

2.6.3 Example 2

Consider the following one state plant model $\mathcal{P} : u \mapsto y$

$$\dot{y} = y^3 + u$$

where the goal is to render $y = 0$ globally asymptotically stable. The perfect state (namely the plant output) is not available due to an unknown output disturbance d, where $d \in L_2$ and $\dot{d} \in L_\infty$. The fact that $d \to 0$ motivates the control law candidate

$$u = -\hat{y}^3 - \alpha\hat{y}$$

with $\alpha > 0$. We show that such an exact cancellation based control law yields only locally stable results, whereas choosing a nonlinear control law for the linearized plant significantly improves the results.

The motivation behind the choice of d above is possible asymptotic estimation error subject to initial condition mismatches. The over-simplicity of this one-state plant should not be misleading, since even if $y(0)$ is known perfectly, the estimator built for plants of the form $\dot{x} = Ax + Bu + F(y)$ with y available, will not necessarily guarantee zero state-estimation error. In fact, if one were to build an estimator

$$\dot{\hat{y}} = u + y^3 + (y - \hat{y})$$

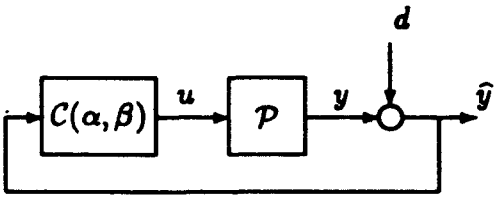

Figure 2.14: Control under perturbed state measurement

and base the control law on $\hat{y}$, by setting $d = \hat{y} - y$, one obtains

$$\dot{d} \;=\; -d \tag{2.1}$$

which implies the L_2 disturbance in the plant states (see Figure 2.14).

Consider the controller of the form

$$C(\alpha,\beta) \;:\; \hat{y} \mapsto u \;\;,\;\; u = -\alpha\hat{y} - \beta\hat{y}^3 \quad .$$

for $\alpha > 0$ and $\beta \geq 1$ and the disturbance d as in (2.1). The dynamics of the resulting closed-loop system in Figure 2.14 is described by

$$\begin{aligned} \dot{y} &= -\alpha(y+d) + y^3 - \beta(y+d)^3 && (2.2)\\ \dot{d} &= -d && (2.1) \end{aligned}$$

Without getting into extensive simulations to obtain the phase-portraits for different α and β values, it is useful to derive some qualitative properties of (2.2) and (2.1) analytically.

For $\alpha > 0$ and $\beta \geq 1$, $(y,d) = (0,0)$ is the only equilibrium point. The Jacobian at $(0,0)$ has eigenvalues $-\alpha$ and -1 , with associated eigenvectors $(y,0)$ and $(y, \frac{1-\alpha}{\alpha}y)$, respectively. Since $d(t)$ cannot change sign, the phase portrait can be decomposed into three invariant sets: $d > 0$, $d = 0$ and $d < 0$; i.e., the trajectories remain exclusively in the set that the initial condition belongs to. There is an odd symmetry in the flows since (y,d) and $(-y,-d)$ satisfy the same differential equations. Hence, it suffices to consider the flow for $d > 0$ since $d = 0$ case is asymptotically stable for all $y(0)$.

The purpose of the exercise is the choice of the nonlinear control determined by β ; although the basin-of-attraction will be affected by the choice of α , the qualitative properties for $\beta = 1$ and $\beta > 1$ are generic. In the following, we will consider the case where $\alpha = 1$, (i.e., the eigenvectors are colinear). Let the Lyapunov function candidate be $V = \frac{1}{2}(y^2 + d^2)$. Evaluating $\dot{V}$ along the solutions of (2.2) and (2.1) , we obtain

$$\dot{V} \;=\; (1-\beta)y^4 - y^2 - (1+3\beta y^2)d^2 - yd(1+3\beta y^2+\beta d^2) \quad . \tag{2.3}$$

From (2.3), one can easily deduce the following:

- $\beta > 1$ $\quad \dot{V}$ is eventually negative, due to the dominating first term in (2.3) . Hence, y remains bounded for any $(y(0), d(0))$. Once d gets sufficiently small , $y \to 0$.

- $\beta = 1$ The first term on the right hand side in (2.3) is zero. The last term changes sign according to (y, d) in the first or second quadrant. Clearly, for any $(y(0), d(0))$ in the first quadrant, the volume V decreases, however, the trajectories might continue into the second quadrant, where the last term becomes positive. In fact, for sufficiently large $d(0)$, the system exhibits finite escape-time.

3 References

[1] B.D.O. Anderson, R.R. Bitmead, C.R. Johnson, Jr., P.V. Kokotovic, R.L. Kosut, I.M.Y. Mareels, L. Praly, and B.D. Riedle, *Stability of Adaptive Systems: Passivity and Averaging Analysis*, MIT Press, 1986.

[2] K.J. Åström and B. Wittenmark, *Adaptive Control*, Addison-Wesley, 1989.

[3] N.N. Bogoliuboff and Y.A. Mitropolskii, *Asymptotic methods in the theory of Nonlinear Oscillators*, Gordon and Breach, New York, 1961.

[4] J.K. Hale, *Ordinary Differential Equations*, Kreiger, Molaban, FL, 1980; originally published (1969), Wiley (Interscience), New York.

[5] A. Isidori, *Nonlinear Control Systems*, 2nd ed., Springer-Verlag, Berlin, FRG, 1989.

[6] A. Isidori and C. Byrnes, "Output regulation of nonlinear systems," *IEEE Trans. on Aut. Contr.*, Vol. AC-32, No. 2, pp.131-140, Feb. 1990.

[7] M. G. Kabuli and R. L. Kosut, "Fast finite-time tracking with saturating actuators," *Proceedings of the 30th IEEE Conference on Decision and Control*, pp. 2883–2884, Brighton, England, December 1991.

[8] M. G. Kabuli and R. L. Kosut, "Adaptive feedback linearization: Implementability and robustness," *Proceedings of the 31st IEEE Conference on Decision and Control*, pp. 251–256, Tucson, Arizona, December 1992.

[9] I. Kanellakopoulos and P. V. Kokotovic, "Observer-based Adaptive Control of Nonlinear Systems Under Matching Conditions," *Proceedings of the American Control Conference*, pp. 549-555, San Diego, CA, May 1990.

[10] I. Kanellakopoulos, P. V. Kokotovic and A. S. Morse, "Systematic Design of Adaptive Controllers for Feedback Linearizable Systems," *IEEE Transactions on Automatic Control*, vol. 36, pp. 1241-1253, November 1991.

[11] R.L. Kosut, D. Meldrum, and G.F. Franklin, "Adaptive control of a nonlinear oscillating system," *Proc. 1989 ACC*, Pittsburgh, PA, June 21-23, 1989.

[12] L. Ljung, *System Identification: Theory for the User* , Prentice-Hall, 1987.

[13] K. Poolla, P. Khargonekar, A. Tikku, J. Krause and K. Nagpal, "A time-domain approach to model validation," *Proceedings of the American Control Conference*, pp. 313–317, Chicago, IL, June 1992.

[14] S. S. Sastry and A. Isidori, "Adaptive Control of Linearizable Systems," *IEEE Transactions on Automatic Control*, vol. 34, pp. 1123-1131, November 1989.

[15] P. D. Shaw, K. R. Haiges, S. M. Rock, J. H. Vincent, A. Emami-Naeini, R. Anex, W. S. Fisk and D. F. Berg, "Design methods for integrated control systems," *Northrop Corporation, Systems Control Technology, Inc., General Electric Company Final Report under Contract AFWAL-TR-88-2061*, for Aero Propulsion Laboratory, Air Force Wright Aeronautical Laboratories, Air Force System Command, Wright-Patterson Air Force Base, June 1988.

[16] M. Tahk and M. Briggs, "An autopilot design technique based on feedback linearization and wind angle estimation for bank-to-turn missile systems," *Proceedings of the AIAA Missile Science Conference*, Monterey, California, November 1988.

[17] M. Tahk, M. Briggs and P. K. Menon, "Applications of plant inversion via state feedback to missile autopilot design," *Proceedings of the 27th IEEE Conference on Decision and Control*, Austin, Texas, December 1988.

[18] M. Vidyasagar, *Control System Synthesis: A Factorization Approach*, MIT Press, 1985.

Appendix A

Appendix A includes a regular paper presented at the 31st IEEE Conference on Decision and Control. An abridged version of the preliminary stages of this work has also been published in the Proceedings of the 1992 Yale Workshop on Adaptive and Learning Systems.

"Adaptive Feedback Linearization: Implementability and Robustness,"
M. Güntekin Kabuli and Robert L. Kosut,
Proceedings of the 31st IEEE Conference on Decision and Control,
pp. 251–256, Tucson, Arizona, December 1992.

Proceedings of the 31st Conference
on Decision and Control
Tucson, Arizona • December 1992

Adaptive Feedback Linearization: Implementability and Robustness

M. Güntekin Kabuli Robert L. Kosut *

Integrated Systems Inc., 3260 Jay Street, Santa Clara, CA 95054-3309

Abstract

The robustness to parameter mismatch in feedback linearization based nonlinear tracking systems is investigated. The certainty-equivalence principle gives rise to four possible feedback configurations: One is the widely used case, where the states are assumed to be available; two others are observer-based; the last one is a model-follower based on a feedforward/feedback implementation using a signal generator. It is noted that the unacceptable transient behaviour of the adaptive tracking scheme is closely related to the sensitivity of the underlying certainty-equivalence based control, which is analyzed through a perturbation approach. Simulations are performed on an example to illustrate the points.

1 Introduction

Consider the following nonlinear tracking problem:

- For a given nonlinear plant with state-space description
$$\begin{aligned} \dot{x} &= f(x,u,\theta) \\ \dot{\theta} &= 0 \\ y &= h(x,u,\theta) \end{aligned},$$
and a given constant reference signal r, determine a feedback law $u = C(y,r)$ such that the closed-loop system is internally stable and the output y asymptotically tracks r.

The parameter θ is clearly uncontrollable. The desired control law has to be expressed in terms of the measured plant variables ; such control laws will be classified as *implementable* . The goal is in fact a robust tracking controller, since performance is achieved despite the uncertainty in the uncontrollable variable θ .

When θ is exactly known, the tracking problem has been solved for special classes of plants that can be rendered linear under algebraic state-feedback and change of coordinates (e.g., [Isi1] and Section II of [Sas1]) .

When θ is unknown, the widely used approach to design an adaptive tracking scheme is the certainty-equivalence principle: the tracking problem is solved as if θ is known and then the above control is based on the estimate $\widehat{\theta}$ (see [Sas1] and the references therein) .

There are two problems with the above approaches. First, the states must all be sensed variables, which is often not the case; hence the controllers are not implementable in our sense. Secondly, certainty-equivalence based designs are not guaranteed to be robust, and hence, the adaptive tracking performance may be unacceptable due to poor transient behaviour, a phenomenon well known in the adaptive linear control (e.g., [And1]) .

*Research supported by AFOSR, Directorate of Aerospace Sciences under contract F49620-90-C-0064 and ARO, Engineering Sciences Division under contract DAAL03-91-C-0011.

A solution to the implementability problem is to use an estimate of the state in the controller. Unfortunately, there is no dual theory of observer design for feedback linearizable systems. Adaptive controllers based on observers have been obtained in the literature for specific classes of nonlinear plants (e.g., under output-matching conditions in [Kan1]) .

Addressing the second problem requires designing a robust nonlinear tracking controller *before* any adaptation is introduced. Hence, prior information on the plant description and the parameter uncertainty are crucial to improve the transient behaviour.

In this paper we consider a special class of nonlinear plants. A direct interpretation of the certainty-equivalence principle gives rise to four possible feedback configurations.

The first one is the widely used case, where the states are assumed to be available. Despite the underlying implementability problem, we address the issue of sensitivity through a perturbation analysis of the approach. Simulations are performed on an example to illustrate the points. Based on this tracking scheme, we derive an adaptive tracking controller. Performance of the tracking scheme is illustrated in an example. Although the responses are bounded, the transients are very large. This unacceptable transient behaviour is closely related to the sensitivity of the underlying (non-adaptive frozen parameter $\widehat{\theta}$) certainty-equivalence based controller.

The other three approaches are all implementable. The state availability assumption is dropped at the expense of global results. Two of the schemes use the state-estimate in two different coordinates. The third is a new model-follower scheme. An example system is used throughout to illustrate the system behaviour using the four schemes.

2 Plant Description

We consider a class of single-input single-output nonlinear plants which can be exactly input-output linearized under algebraic state-feedback and change of coordinates. The class under consideration has no zero dynamics. Specifically, we assume the following:

1. The plant dynamics has the state-space description
$$\begin{aligned} \dot{x} &= Ax + Bu + f_0(x) + F_1(x)\theta \\ y &= c^T x \end{aligned} \qquad (1)$$
where $x \in \mathbb{R}^n$ is the state, $u \in \mathbb{R}$ is the scalar control input, $y \in \mathbb{R}$ is the scalar sensed output.

2. The matrices A and B are in the Brunowsky canonical form. $c^T := [\,1\,0\,0\,\ldots\,0\,]$.

3. The smooth nonlinear functions $f_0 : \mathbb{R}^n \to \mathbb{R}^n$ and $F_1 : \mathbb{R}^n \to \mathbb{R}^{n\times p}$ are known and have the lower-triangular forms

CH3229-2/92/0000-0251$1.00 © 1992 IEEE

$f_{0(i)}(x) = \tilde{f}_{0(i)}(x_1, x_2, \ldots, x_i)$ and $F_{1(i,j)}(x) = \tilde{F}_{1(i,j)}(x_1, x_2, \ldots, x_i)$ for $i = 1, \ldots, n$, $j = 1, \ldots, p$.

4. $\theta \in \mathbb{R}^p$ is a vector of *unknown* constant parameters.

2.1 Remarks

For the above plant description, there exists a possibly parameter dependent, coordinate transformation, $\xi = \Phi(x, \theta)$, where $\Phi(\cdot, \theta)$ is a diffeomorphism for all θ . Under the coordinate transformation Φ , (1) can be equivalently described by

$$\begin{aligned} \dot{\xi} &= A\xi + B[u + g_0(x) + G_1(x)\psi] \\ y &= c^T\xi \end{aligned} \tag{2}$$

where the over-parametrization ψ consists of entries of appropriate tensor products of θ .

The class of plants under consideration are transformable to $y^{(n)} = u + g_0(x) + G_1(x)\psi$; hence, they are state-dependent perturbations of a string of n-integrators.

For notational convenience, we will refer to the linear part in (2), i.e., the triple (I, A, B) as the linear plant P . Let

$$\mathcal{F}(x) := g_0(x) + G_1(x)\psi \quad . \tag{3}$$

This class of plants satisfies the parametric strict-feedback condition in [Kan2] ; hence, provided that the state x is available for feedback, one can obtain a globally adaptive tracking system for the plant in (1) using the procedure in [Kan2] .

The class of plants under consideration include the so-called benchmark example , where $n = 3$, $p = 1$, $f_0(x) = 0$ and $F_1(x) = [f(x_1)\ 0\ 0]^T$, where $f(\cdot)$ is not necessarily Lipschitz in x_1 .

We will denote "state-x is available for feedback" rather than "state is available for feedback" , in order to emphasize the specific coordinate the dynamics is described in. Note that even if state-x in (1) is available, state-ξ is not available, since it depends on a θ-dependent transformation where θ is unknown.

Whenever we refer to a stable map, the map is causal and bounded-input bounded-output stable (defined over an appropriate extended space). With a slight abuse of notation, a stable proper transfer function $h(s)$ will be denoted as h in the input-output description where $hG(x)$ will denote the time-domain waveform obtained by convolving the impulse response corresponding to $h(s)$ and the signal $G(x)$. Parantheses will be used where ambiguity arises. Unless specifically emphasized, factorizations denote proper stable factorizations.

2.2 Example

A simple third-order example, satisfying the conditions in Section 2, is used to illustrate certain points throughout the paper. Consider

$$\begin{aligned} \dot{x}_1 &= x_2 + \theta f(x_1) \\ \dot{x}_2 &= x_3 \\ \dot{x}_3 &= u \\ y &= x_1 \quad . \end{aligned} \tag{4}$$

Since we are interested in an input-output approach, all initial conditions in the simulations are assigned as zero.

Candidates for the function $f(\cdot)$ that we have used are:

- $f(x_1) = -\tanh(\alpha x_1)$, motivated by a simple saturating friction nonlinearity. Note that although f is Lipschitz, the corresponding G_1 is not.
- $f(x_1) = -x_1^2$, following the benchmark problem in [Kan2].
- $f(x_1) = -x_1^2/(\alpha x_1^2 + 1)$.

The function f used in a particular simulation will be emphasized. We introduce the following, for future reference.

$$P := \frac{1}{s^3}\begin{bmatrix} 1 & s & s^2 \end{bmatrix}^T$$

$$\Phi(x) = \begin{bmatrix} x_1 \\ x_2 + \theta f(x_1) \\ x_3 + \theta x_2 f^{(1)}(x_1) + \theta^2 f(x_1) f^{(1)}(x_1) \end{bmatrix} =: \xi$$

$$\Phi^{-1} : \xi \mapsto \begin{bmatrix} \xi_1 \\ \xi_2 - \theta f(\xi_1) \\ \xi_3 - \theta \xi_2 f^{(1)}(\xi_1) \end{bmatrix}$$

$$g_0(x) := 0$$

$$G_1(x) := \begin{bmatrix} x_2^2 f^{(2)}(x_1) + x_3 f^{(1)}(x_1) \\ 2x_2 f(x_1) f^{(2)}(x_1) + x_2 (f^{(1)}(x_1))^2 \\ f(x_1)(f^{(1)}(x_1))^2 + f^2(x_1) f^{(2)}(x_1) \end{bmatrix}^T$$

$$\psi := \begin{bmatrix} \theta & \theta^2 & \theta^3 \end{bmatrix}^T$$

Note that for this example,

$$\begin{aligned} G_1(x)\psi &= (f^{(2)}(\xi_1)\xi_2^2 + f^{(1)}(\xi_1)\xi_3)\theta \\ &=: \tilde{G}_1(\xi)\theta \quad , \end{aligned} \tag{5}$$

which emphasizes the issue of overparametrization in different coordinates.

Another observation which becomes useful in the perturbation description is the map $(\hat{\Phi}\Phi^{-1} - I)$, where

$$\hat{\Phi}\Phi^{-1}(\xi) = \hat{\Phi}\begin{bmatrix} \xi_1 \\ \xi_2 - \theta f(\xi_1) \\ \xi_3 - \theta \xi_2 f^{(1)}(\xi_1) \end{bmatrix}$$

$$= I(\xi) + (\hat{\theta} - \theta)\begin{bmatrix} 0 \\ f(\xi_1) \\ \xi_2 f^{(1)}(\xi_1) + \hat{\theta} f(\xi_1) f^{(1)}(\xi_1) \end{bmatrix} . \tag{6}$$

3 State-x Available

3.1 On Sensitivity of State-x Based Stabilization

The contents of this particular subsection focuses on a slight generalization of the class in Section 2 , where the input u need not be scalar.

Consider the input u to state-x map described by (1) or equivalently, by (2) . Under a change of coordinates (Φ) , the input u to state-ξ map can be rendered linear under an algebraic state-feedback $\mathcal{F}$ (see (3)) . Hence u to state-x map can be realized as in the dashed-box in Figure 1 .

The map from v to ξ is linear (time-invariant finite dimensional). Let $\xi = Pv$. Since P admits coprime factorizations, $P = ND^{-1} = \tilde{D}^{-1}\tilde{N}$ with $\begin{bmatrix} \tilde{U} & \tilde{V} \\ -\tilde{D} & \tilde{N} \end{bmatrix}\begin{bmatrix} N & -V \\ D & U \end{bmatrix} = I$, where all eight maps in the above identity are stable.

The nonlinear map Φ is stable and its inverse is stable.

The algebraic map $\mathcal{F}$ is stable. In fact, for the subsequent derivations in this subsection, Φ and $\mathcal{F}$ need not be algebraic.

Note that, the input to state-x map in Figure 1 can be expressed as

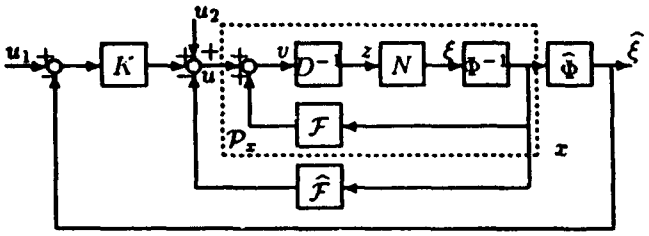

Figure 1: Stabilizing scheme based on the estimates $\hat{\mathcal{F}}$ and $\hat{\Phi}$

$$\mathcal{P}_x = \Phi^{-1}N(D - \mathcal{F}\Phi^{-1}N)^{-1} \quad (7)$$
$$= (\tilde{D}\Phi - \tilde{N}\mathcal{F})^{-1}\tilde{N} \quad (8)$$

where

$$(\tilde{U}\Phi + \tilde{V}\mathcal{F})(\Phi^{-1}N) + (\tilde{V})(D - \mathcal{F}\Phi^{-1}N) = I \quad (9)$$
$$(\tilde{D}\Phi - \tilde{N}\mathcal{F})(\Phi^{-1}V) + (\tilde{N})(U + \mathcal{F}\Phi^{-1}V) = I \quad (10)$$

Note that, (9)-(10) imply that (7)-(8) are in fact nonlinear right- and left-coprime factorizations of $\mathcal{P}_x$, respectively. The equations (9) and (10) also describe a stabilization scheme based on undoing the nonlinearities, since a stabilizing $C : x \mapsto u$ is given by

$$C = -K\Phi - \mathcal{F} \quad ,$$

where $v = -K\xi$ stabilizes P.

In order to incorporate the θ dependence in the u to x map, consider Φ and $\mathcal{F}$ both functions of θ whereas P is independent of θ. Note that such an assumption is not restrictive, since typically the choice of coordinates and algebraic state-feedback is constructed to render P as a string of integrators (in each channel). From now on, P and its associated terms in the Bezout-identity will be considered as θ-independent. The θ dependence in Φ and $\mathcal{F}$ will be emphasized by introducing the $\hat{\ }$-versions when they're determined by the parameter estimate $\hat{\theta}$.

We now can express the standard stabilization scheme based on certainty-equivalence approach in terms of the maps introduced so far. Since θ is not exactly known, the control law from x to u is realized as

$$u = K(\hat{\xi}_r - \hat{\Phi}(x)) - \hat{\mathcal{F}}(x) \quad , \quad (11)$$

where $\hat{\xi}_r$ denotes the desired reference in terms of the state-$\hat{\xi}$ (see Figure 1). In other words, when $\theta = \hat{\theta}$, the tracking performance is determined by

$$\xi = Pv$$
$$v = K(\hat{\xi}_r - \xi) \quad .$$

Note that the tracking scheme in (11) can be equivalently represented by the control law,

$$\hat{v} = K(\hat{\xi}_r - \hat{\xi}) \quad ,$$

where K is a $\hat{\xi}_r$-tracking compensator for $P : v \mapsto \xi$, and $\hat{v}$, $\hat{\xi}$ are as shown in Figure 2.

Note that the stable feedback perturbation in Figure 2 can be expressed as $(\mathcal{F} - \hat{\mathcal{F}})\Phi^{-1}$, since $x = \Phi^{-1}(\xi)$ is available, although Φ and ξ are not. As long

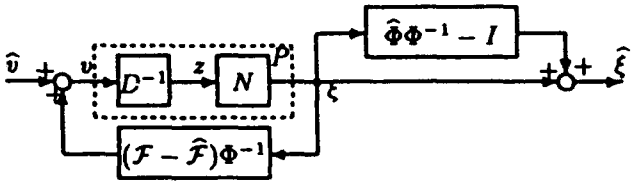

Figure 2: Perturbation of $P : v \mapsto \xi$ under θ mismatch

as the feedback law from $\hat{\xi}$ to $\hat{v}$ is chosen as a linear time-invariant K stabilizing $P = ND^{-1}$, one obtains the precise conditions under which the certainty-equivalence based control law can withstand θ perturbations. Before stating the conditions, we will adopt the following definition.

- Let K stabilize P (i.e., $K = \tilde{V}^{-1}\tilde{U}$ and $P = ND^{-1}$, where $\tilde{U}N + \tilde{V}D = I$). K is said to stabilize the perturbed plant in Figure 2 iff the control law $\hat{v} = u_2 + K(u_1 - \hat{\xi})$ yields a stable $(u_1, u_2) \mapsto z$, where z denotes the pseudo-state in Figure 2 (see also Figure 1).

With this definition, one can work out the pseudo-state equation to derive the necessary and sufficient condition for K to robustly stabilize the perturbed v to ξ map, i.e.,

$$(I + \begin{bmatrix} \tilde{V} & \tilde{U} \end{bmatrix} \begin{bmatrix} (\hat{\mathcal{F}} - \mathcal{F})\Phi^{-1} \\ \hat{\Phi}\Phi^{-1} - I \end{bmatrix} N) \quad (12)$$

has a stable inverse. Note that P can be stabilized using only its first output, i.e., there exist $\tilde{U} =: [\tilde{U}_1 \; 0 \; 0 \; \ldots \; 0]$, such that $\tilde{U}N + \tilde{V}D = I$. Hence using a dynamic feedback compensator of the form $K =: [C \; 0 \; 0 \; \ldots \; 0]$, C stabilizes P; moreover, the map in (12) further simplifies to $(I + \tilde{V}(\hat{\mathcal{F}} - \mathcal{F})\Phi^{-1}N)$ since $c^T(\hat{\Phi}\Phi^{-1} - I) = 0$.

Typical robustness results (small-gain, passivity based sufficient conditions) can be utilized together with assumptions on the nonlinear post-multiplicative and feedback perturbations in (12) (such as sector bounded nonlinearities, linear or multilinear θ dependence etc.) to generate classes of systems for which (12) can be justified. However, we are not interested in further restricting the set of plants under investigation for the sake of forcing some sufficient conditions. For the simple example in Section 2.2, even if the nonlinearity $f(\cdot)$ is chosen to be globally Lipschitz, the same is no longer true for $\mathcal{F}$.

3.2 Sensitivity to e_θ : Simulation

The example in Section 2.2 with $f(x_1) = -x_1^2$ is used for the following simulation.

Recall that, since $\xi_1 = x_1 = y$, from (6), $c^T(\hat{\Phi}\Phi^{-1} - I) = 0$. Hence, by choosing a dynamic compensator C from y to $\hat{v}$, the error introduced by the output multiplicative term in Figure 2 is avoided.

The compensator $C : y \mapsto \hat{v}$ is chosen as an $\mathcal{H}_2$-optimal compensator for $1/s^3$ for a particular choice of weights. Throughout the simulations, $C(s) = \frac{70.222s^2 + 40.055s + 10}{s^3 + 9.5219s^2 + 35.3333s + 66.6297}$.

The sensitivity of the closed-loop to $e_\theta := \theta - \hat{\theta}$ is illustrated as follows: The parameter θ is chosen as

$\theta = 1$. For a unit-step reference input the parameter estimate $\hat{\theta}$ is perturbed about the nominal value 1 . When $\theta = \hat{\theta}$, the closed-loop system exhibits the desired tracking response of a linear system. When $\hat{\theta}$ is perturbed to 1.0025 and 1.005 , the tracking performance of the loop is shown in Figure 3 .

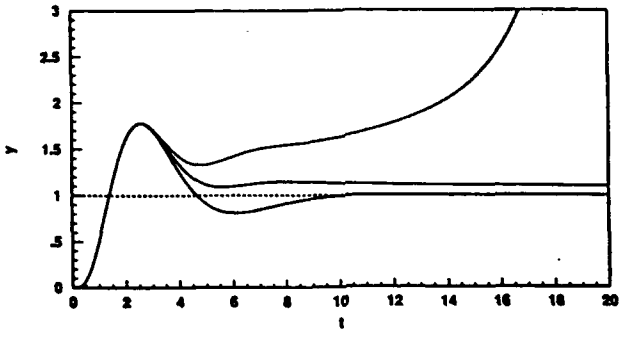

Figure 3: Sensitivity of certainty-equivalence based design using state-x for $\theta = 1$, $\hat{\theta} = 1$, 1.0025 , 1.005 .

Clearly, within 0.5% relative error, the asymptotic tracking property is lost and the system goes unstable. An adaptation law based on this sensitive closed-loop is bound to exhibit unsatisfactory transient behaviour even if asymptotic tracking is achieved by parameter adaptation. Note that, Figure 3 shows the closed-loop responses for *frozen* $\hat{\theta}$ values. Hence, one should definitely avoid very slow adaptation.

3.3 Adaptation

For the plant description in Section 2 , provided that the state-x is also available for exact linearization, one can bring an input-output approach to a particular case of certainty-equivalence based adaptive control design.

We now outline the design procedure:

1. For the class of plants in Section 2 , determine g_0 and G_1 , reducing zero columns of G_1 (if any) to cut down on unnecessary overparametrization in ψ .

2. Design a stable stabilizing compensator $C(s)$ for $1/s^n$; i.e., $C =: n_c/d_c$, $1/s^n =: n_p/d_p$ and $n_p n_c + d_p d_c = 1$.

3. An adaptive tracking control law candidate is determined by applying the control

$$u = C(r-y) - g_0(x) - (G_1 x)\hat{\psi} \quad , \qquad (13)$$

where the parameter estimate $\hat{\psi}$ is updated using the error equation

$$y - n_p n_c r = d_c n_p((G_1 x)e_\psi) \quad , \qquad (14)$$

so that $y \rightarrow n_p n_c r$. ($e_\psi = \psi - \hat{\psi}$ and r denotes a reference signal that tracks a step input.)

Note that $(y - n_p n_c r)$ in (14) denotes the error between the plant output and the ideal tracking performance (if the nonlinear cancellations were exact) .

Consider the nonlinear plant described in Section 2 shown in Figure 1. For the scalar input case, let $D = d_p$.

The pseudo-state equations can be written as

$$\begin{aligned} d_p z &= u + g_0(x) + G_1(x)\psi \\ Nz &= \xi \\ \Phi x &= \xi \\ y &= \xi_1 \quad , \end{aligned}$$

where N and d_p are stable; $c^T N =: n_p$ and (n_p, d_p) is a right coprime factorization of $1/s^n$. Since n_p is minimum-phase, $n_p d_p^{-1}$ is strongly stabilizable. Hence there exist n_c,d_c with d_c^{-1} stable, satisfying $n_c n_p + d_c d_p = 1$.

Since N is strictly proper, $\mathcal{G}$ is strictly causal, where

$$\begin{aligned} \mathcal{G} &= \mathcal{G}_0 + (\mathcal{G}_1(\cdot))\psi \\ \mathcal{G}_0 z &= g_0 x \qquad (15) \\ \mathcal{G}_1 z &= G_1 x \quad . \qquad (16) \end{aligned}$$

Hence,

$$d_p z = u + \mathcal{G} z$$

describes a well-posed u to z map. Since Φ and Φ^{-1} are stable maps and (n_p, d_p) is a right-coprime pair, the plant can be equivalently represented by the following pseudo-state equation

$$\begin{aligned} d_p z &= u + \mathcal{G} z \\ n_p z &= y \quad . \end{aligned}$$

Note that although z is not available, $\mathcal{G}_0 z$ and $\mathcal{G}_1 z$ are available since state-x is available ((15),(16)) .

Hence the plant description from u to y can be expressed as

$$y = n_p (d_p - \mathcal{G})^{-1} u \quad .$$

Now apply the certainty equivalence based control law

$$u = u_2 + \frac{n_c}{d_c}(u_1 - y) - \mathcal{G}_0 z - (\mathcal{G}_1 z)\hat{\psi}$$

where u_1 and u_2 denote the exogenous additive inputs at the plant input and output in the standard unity-feedback system, respectively.

For $u_2 = 0$, $u_1 = r$, where r denotes the desired reference, we obtain

$$y - n_p n_c r = d_c n_p((\mathcal{G}_1 z)e_\psi) \quad .$$

Since $d_c n_p$ is minimum-phase, one can utilize an augmented error scheme to update e_ψ .

In order to cut down on the number of states introduced by the filters in the augmented error scheme, we use the filtered error e_y ,

$$e_y := d_c^{-1}(y - n_p n_c r) \quad . \qquad (17)$$

Since n_p is minimum-phase, one can adapt $\hat{\psi}$ using the error form

$$e_y = n_p((\mathcal{G}_1 z)e_\psi) \quad . \qquad (18)$$

Since $(d_c d_p)(0) = 0$, when cancellation is exact, step inputs can be asymptotically tracked.

We now derive the update law, based on the error equation in (18) . Since it utilizes the standard augmented error scheme, we briefly outline the steps.

Since n_p is minimum-phase and strictly proper, it can always be expressed as $n_p =: h_1 h_2$, where h_1 is strictly positive real, strictly proper and h_2 is proper

stable. Note that $h_1 = \frac{1}{s+1}$ and $h_2 = (s+1)n_p$ will always work, since n_p is strictly proper. However, to cut down on the number of states introduced by filtering by h_2 in the augmented error implementation, it is advisable to factor out a strictly positive real factor of n_p, instead.

For ease of notation, let $W := \mathcal{G}_1 z$. Then (18) can be written as $e_y = h_1 h_2 (W e_\psi)$. After adding, subtracting terms and using the fact that $\dot{\psi} = 0$, we obtain

$$\eta = h_1((h_2 W)e_\psi) \quad ,$$

where $\eta := e_y - h_1((h_2 W)\widehat{\psi} - h_2(W\widehat{\psi}))$. Since h_1 is strictly positive real, the update law

$$\dot{\widehat{\psi}} = \gamma(h_2 W)^T \eta \quad , \quad \gamma > 0$$

guarantees that $\eta \in \mathcal{L}_2 \cap \mathcal{L}_\infty$ and $e_\psi \in \mathcal{L}_\infty$. Provided that the closed-loop signals are bounded, $W \in \mathcal{L}_\infty$; hence, $\eta \to 0$, $\dot{\widehat{\psi}} \to 0$ and $e_y \to 0$. This concludes that set point tracking is achieved in the limit provided that the closed-loop signals remain bounded.

3.3.1 Adaptive Tracking: Simulation

The adaptation scheme above is applied to the example in Section 2.2 for two choices of f . In both adaptive schemes, the closed-loop signals remain bounded; hence asymptotic tracking is achieved. However, the transient responses are unacceptable. Note that in both cases, even without adaptation, state-x based certainty-equivalence control performance was extremely sensitive to constant parameter errors.

- $f(x_1) = -x_1^2/(\alpha x_1^2 + 1)$, $\alpha = 0.05$, $\gamma = 10$, reference $r = 1$, $\theta = 1$. This function approximates $f(x_1) = -x_1^2$ reasonably for $|x_1| \leq 2$. The tracking performance is shown in Figure 4.
- $f(x_1) = -\tanh(\alpha x_1)$, $\theta = -1$, $\alpha = 4$, $\gamma = 1$, reference $r = 0.1$. The tracking performance is shown in Figure 5.

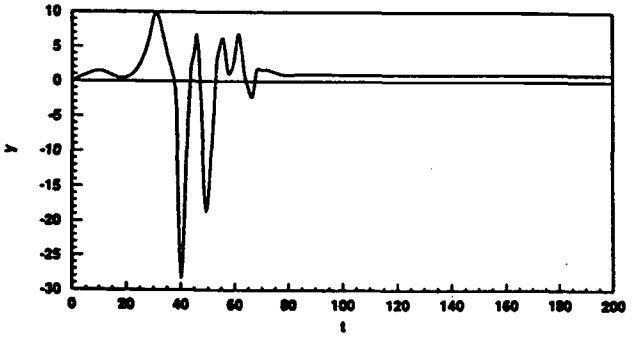

Figure 4: Asymptotic tracking of $r = 1$ from zero initial conditions

4 On Implementable Certainty-Equivalence Based Controllers

Recall that the example in Section 2.2 can be expressed in x or ξ coordinates as in (1) and (2), respectively. Note also that, due to (5), there is no need for overparametrization in the ξ coordinates.

If the parameter vector θ and either the state x or ξ are known, then either the control

$$u = v - \theta \widetilde{G}_1(\xi) \qquad (19)$$

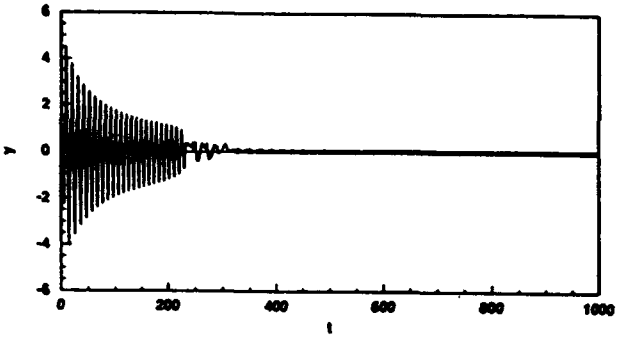

Figure 5: Asymptotic tracking of $r = 0.1$ from zero initial conditions

or, in terms of the state x, the control

$$u = v - G_1(x)\psi \qquad (20)$$

provides exact *input-output linearization*. That is, the system $v \mapsto y$ is linear time-invariant, where

$$\begin{aligned} \dot{\xi} &= A\xi + Bv \\ y &= \xi_1 \end{aligned}$$

Let $C(s)$ be the same stabilizing compensator (for (c^T, A, B)) as in Section 3.2 . Hence $v = C(r - y)$, where r denotes the desired reference, achieves the desired tracking performance when $\widehat{\theta} = \theta$.

Since the parameter vector θ and neither state x nor ξ are known, it is natural to replace them in (19) and (20) with estimates $\widehat{\theta}$, $\hat{x}$, and $\hat{\xi}$. This is the *certainty equivalence principle*. As it does make a difference which observer state is used, we consider them separately. As in Section 3.2 , the following simulations are based on $f(x_1) = -x_1^2$.

4.1 Observer in the State-x

The control law is

$$\begin{aligned} \dot{\hat{x}} &= (A - Lc^T)\hat{x} + Bu + F_1(\hat{x})\hat{\theta} + Ly \\ u &= v - G_1(\hat{x})\widehat{\psi} \quad , \end{aligned} \qquad (21)$$

where $(A - Lc^T)$ is strictly Hurwitz. Since all simulations are performed with zero initial conditions, provided that $\widehat{\theta} = \theta$, the nominal performance is identical to that of the linear equivalent.

The sensitivity of the closed-loop to $e_\theta := \theta - \widehat{\theta}$ is illustrated as follows: The parameter θ is chosen as $\theta = 1$. For a unit-step reference input the parameter estimate $\widehat{\theta}$ is perturbed about the nominal value 1 . When $\widehat{\theta}$ is perturbed to 1.1 and 1.2 , the tracking performance of the loop is shown in Figure 6 .

4.2 Observer in the State-ξ

The control law is

$$\begin{aligned} \dot{\hat{\xi}} &= (A - Lc^T)\hat{\xi} + B[u + \widehat{\theta}\widetilde{G}_1(\widehat{\xi})] + Ly \\ u &= v - \widehat{\theta}\widetilde{G}_1(\widehat{\xi}) \quad , \end{aligned} \qquad (22)$$

where $(A - Lc^T)$ is strictly Hurwitz. Since all simulations are performed with zero initial conditions, provided that $\widehat{\theta} = \theta$, the nominal performance is identical to that of the linear equivalent.

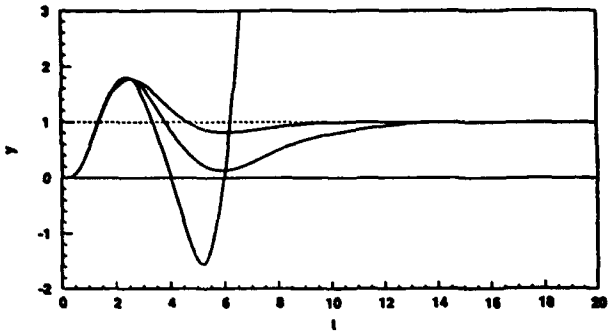

Figure 6: Sensitivity of certainty-equivalence based design using the estimate of state-x for $\theta = 1$, $\widehat{\theta} = 1$, 1.1 , 1.2 .

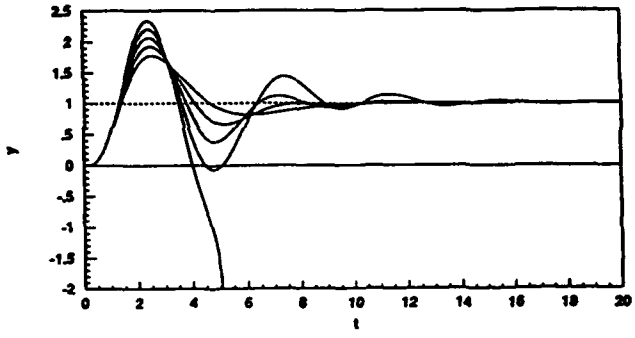

Figure 7: Sensitivity of certainty-equivalence based design using the estimate of state-ξ for $\theta = 1$, $\widehat{\theta} = 1$, 1.25 , 1.5 , 1.75 , 2 .

For a unit-step reference, $\widehat{\theta}$ is perturbed 1.25, 1.5, 1.75 and 2 ; the tracking performance of the loop is shown in Figure 7 .

4.3 Model-Follower

This feedback-feedforward control scheme is based on a locally stable unity-feedback system. For the given nonlinear plant $\mathcal{P} : u \mapsto y$, let $C_{\mathcal{P}}(s)$ locally stabilize the plant in the unity-feedback system about the reference r . A model is used to generate the feedforward signals. The model is a copy of the plant description, where θ is replaced by $\widehat{\theta}$. Since all states are available for this model, exact linearization can be performed. Let $C(s)$ be the compensator that is being used so far in the previous three certainty-equivalence based designs. Subscript-m denotes the model variables.

The control law is (see Figure 8) :

$$\begin{aligned} \dot{\xi}_m &= A\xi_m + Bv_m \\ y_m &= c^T\xi_m \\ v_m &= C(r - y_m) \\ u_m &= v_m - \widehat{\theta}\widetilde{G}_1(\xi_m) \\ u &= u_m + C_{\mathcal{P}}(y_m - y) \quad . \end{aligned} \tag{23}$$

For the specific example, $C_{\mathcal{P}} = C$ achieved local stabilization about the unit-step reference. $\widehat{\theta}$ is perturbed to 1.25, 1.5, 1.75 , 2 , 2.5 , 2.75 and 3 ; the tracking performance of the loop is shown in Figure 9 . Note that this scheme exhibits the least sensitive tracking design.

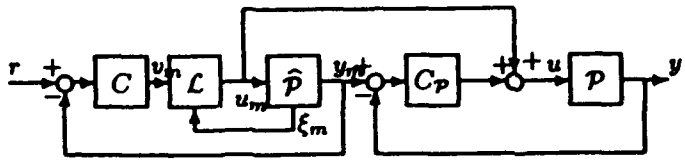

Figure 8: Model-follower described by (23), where $\mathcal{L}(v_m, \xi_m) := v_m - \widehat{\theta}\widetilde{G}_1(\xi_m)$.

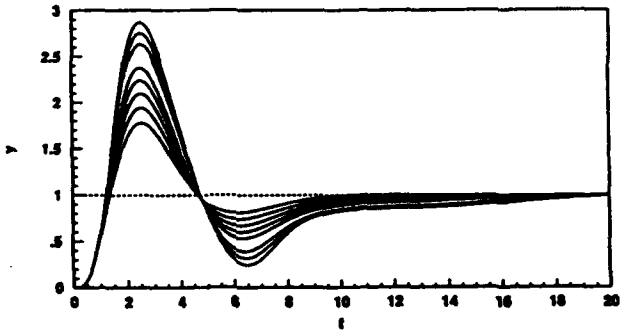

Figure 9: Sensitivity of the model-follower based certainty-equivalence design for $\theta = 1$, $\widehat{\theta} = 1$, 1.25 , 1.5 , 1.75 , 2 , 2.5 , 2.75 , 3 .

5 Concluding Remarks

An input-output approach has yielded some insight into robustness of feedback linearizable schemes under parameter mismatch. Our simulations of adaptive nonlinear systems show a phenomenon familiar in adaptive linear systems. Namely, even though the system is theoretically globally stable, the transient can be quite large. The problem is inherent in the parameter sensitivity of the system when the adaptation is frozen. The observer-based and model-follower schemes are most likely more robust to parameter changes then the full-state available scheme, which in general, is not implementable unless the states are measured.

References

[And1] B. D. O. Anderson, R. R. Bitmead, C. R. Johnson, Jr., P. V. Kokotovic, R. L. Kosut, I. M. Y. Mareels, L. Praly and B. D. Riedle, *Stability of Adaptive Systems: Passivity and Averaging Analysis* , MIT Press, 1986.

[Isi1] A. Isidori, *Nonlinear Control Systems* , Springer-Verlag, 1989.

[Kan1] I. Kanellakopoulos and P. V. Kokotovic, "Observer-based Adaptive Control of Nonlinear Systems Under Matching Conditions," *Proceedings of the American Control Conference*, pp. 549-555, San Diego, CA, May 1990.

[Kan2] I. Kanellakopoulos, P. V. Kokotovic and A. S. Morse, "Systematic Design of Adaptive Controllers for Feedback Linearizable Systems," *IEEE Transactions on Automatic Control*, vol. 36, pp. 1241-1253, November 1991.

[Sas1] S. S. Sastry and A. Isidori, "Adaptive Control of Linearizable Systems," *IEEE Transactions on Automatic Control*, vol. 34, pp. 1123-1131, November 1989.

Appendix B

Appendix B includes a regular paper presented at the 1993 Automatic Control Conference.

"On Feedback Linearizable Plants,"
M. Güntekin Kabuli and Robert L. Kosut,
Proceedings of the American Control Conference,
pp. 1186–1190, San Francisco, June 1993.

Proceedings of the
American Control Conference
San Francisco, California • June 1993

On Feedback Linearizable Plants

M. Güntekin Kabuli Robert L. Kosut *

Integrated Systems Inc., 3260 Jay Street, Santa Clara, CA 95054-3309

Abstract

An input-output approach is used to investigate stabilization of a class of nonlinear plants that can be rendered linear time-invariant under nonlinear stable dynamic feedback. Results are obtained for the standard unity-feedback configuration subject to bounded disturbances. It is shown that the design method based on applying the inverse transformation on *any* stabilising controller for the transformed linear time-invariant plant, does not necessarily yield a stabilising controller for the nonlinear plant. Conditions under which the method is justified are derived.

1 Introduction

Due to the relative ease of solving control problems associated with finite-dimensional linear time-invariant (LTI) plants, the class of nonlinear plants that can be rendered LTI by algebraic state-feedback has received considerable attention in the literature (e.g., [Isi1, Sas1, Kan1] and references therein) . This transformation based approach provides one of the few systematic means of designing nonlinear control laws and has been applied to numerous research problems involving stabilisation, tracking, adaptive stabilization and adaptive tracking. While most of these applications might be valid nominal design approaches, the stability of resulting closed-loop systems subject to plant uncertainties and/or disturbance models has not received comparable attention.

Towards the goal of establishing robust control design methodologies for classes of nonlinear plants, a crucial step is guaranteeing stability when the system is subject to persistently exciting bounded disturbances and determining bounds on such disturbances for which stability is guaranteed. In other words, design methods and the subsequent analyses must be able to justify stability (be it local or global) in the presence of sensor and/or actuator noise, even before bringing in more demanding robustness to plant uncertainties.

In this paper, motivated by the class of nonlinear plants that can be rendered LTI under nonlinear algebraic state-feedback, we focus on a particular class of nonlinear plants that can be rendered LTI under nonlinear *stable*, possibly dynamic, feedback. We study the stabilisation of this particular class of nonlinear plants. The study is based on an input-output framework, where the closed-loop results are stated for the standard unity-feedback configuration subject to bounded actuator and sensor disturbances [Des1] .

The results are organised as follows. The relationships between the graphs of the nonlinear plant and its transformed LTI counterpart are derived; the fact that the bounded input-output pairs of the two maps are related by stable maps motivates the generally adopted design procedure based on undoing the nonlinearities, which consists of the following steps:

1. transform the nonlinear plant to an LTI one,
2. design a stabilising controller (possibly nonlinear) for the LTI plant and
3. using the inverse transformation and the designed controller for the LTI plant, determine the transformed controller for the nonlinear plant.

It is shown that this straightforward three step procedure is *not* a unified stabilising control design method for the class of plants at hand *when the plant is subject to bounded actuator/sensor disturbances* . In other words, given any member of the particular class of plants under study, taking the three steps mentioned above does not necessarily guarantee a stabilising controller. As might be expected, the problem arises due to the second step of the design procedure, since it inherently assumes that the design for the transformed LTI plant and the nonlinear plant are separate problems. In other words, *any* stabilising controller for the LTI plant may not yield a stabilising controller in the third step. Subsequent results formalise this issue and state conditions under which such a design approach is justified. While the notion of incremental stability, which generalises the properties of linear stable maps, can be easily imposed to guarantee sufficient conditions for the method to work in general, the extreme conservatism in expecting *any* controller in the second design step to work is shown by establishing that incremental stability has to be *necessary* , as well. Unless such restrictions happen to be satisfied for the specific problem at hand, all of these cautionary results imply the following: The design problem for the transformed LTI plant need not be decoupled from the original nonlinear design problem; hence, one should not rule out intentionally nonlinear controller design for the transformed LTI plant. Although this might seemingly defy the purpose of the transformation, since the transformed design problem is yet another nonlinear control design problem, it also emphasises the need for more results in nonlinear control design for LTI plants, before nonlinear plants are transformed to linear ones. Moreover, despite the global linearising transformation, one might end up with only a locally stable interconnection. Simple examples with analytical derivations are used to emphasise the points.

1.1 Notation and Preliminaries

• All nonlinear maps in this study are causal, multi-input multi-output and defined over appropriate products of extended $L_\infty[0,\infty)$ spaces. For a thorough treatment of general extended spaces within the input-output approach to nonlinear systems, see e.g., [Des1] .

*Research supported by ARO, Engineering Sciences Division under contract DAAL03-91-C-0011 and AFOSR, Directorate of Aerospace Sciences under contract F49620-90-C-0064.

For notational convenience, for functions from $\mathbb{R}_+$ to $\mathbb{R}^n$, the associated set of bounded signals and the extended space will ve denoted by L_∞^n and $L_{\infty e}^n$, respectively.

While most of the observations in this study do generalize to other extended spaces, the particular choice of sup bounded functions on $\mathbb{R}_+$ is motivated by studying the stability properties of nonlinear interconnections subject to persistently exciting disturbances.

An n_i-input n_o-output causal nonlinear map $\mathcal{P}$ will be considered as

$$\mathcal{P} : \mathcal{U} \subset L_{\infty e}^{n_i} \rightarrow L_{\infty e}^{n_o} \quad ,$$

where $\mathcal{U}$ denotes the domain. The extended space is a means of incorporating unbounded signals in the study; however, one must note that although $L_\infty \subset L_{\infty e}$, $(L_\infty)^C \setminus L_{\infty e} \neq \emptyset$, where $(\cdot)^C$ denotes the complement of the set with respect to the set of all functions on $\mathbb{R}_+$. The nonempty intersection arises due to discontinuities which are not jump-discontinuities. The scope of the extended spaces does not cover signals which exhibit "finite escape time"; hence the plant description over a strictly proper subset of the input extended space might be necessary. Hence, L_∞^n describes the set of bounded signals and $L_{\infty e} \setminus L_\infty$ denotes the set of unbounded signals (unbounded at infinity).

- Calligraphic capital letters will be used to denote nonlinear maps. Italic capital letters will denote linear time-invariant maps that admit finite-dimensional state-space descriptions; for this class, with a slight abuse of notation, the map and its associated transfer function representation will be used interchangeably. In the case that italic letters are used for nonlinear algebraic maps, parentheses will be included to emphasize the evaluation (i.e., Ax vs. $F(x)$). For two nonlinear causal maps $\mathcal{F}$ and $\mathcal{G}$ the map $\mathcal{FG}$ will denote the composition of the two maps.
- In an input-output approach to the analysis and design of nonlinear interconnections, the notions of boundedness and stability are crucial for subsequent results. Unlike the finite-dimensional linear time-invariant case, most of these properties depend on the particular framework. The following four definitions set up the particular framework in this paper. For a treatment of related topics in fractional representations of nonlinear casual maps and stability of nonlinear interconnections see e.g., [Ham1, Ver1, Vid1, Kab1] and references therein.
- The set of all input output pairs of a given map does admit a special partitioning which exhibits particular properties.

Definition 1 (graph of $\mathcal{P}$, $\mathcal{G}(\mathcal{P})$)
For a given map $\mathcal{P} : \mathcal{U} \subset L_{\infty e}^{n_i} \rightarrow L_{\infty e}^{n_o}$, the graph of $\mathcal{P}$ is denoted by $\mathcal{G}(\mathcal{P})$, where
$\mathcal{G}(\mathcal{P}) = \{ (u, \mathcal{P}u) \mid u \in \mathcal{U} \} \subset \mathcal{U} \times \mathcal{P}(\mathcal{U})$. $\diamond$

Note that, $\mathcal{G}(\mathcal{P})$ admits the following unique partitioning
$\mathcal{G}(\mathcal{P}) = \mathcal{G}_{BB}(\mathcal{P}) \cup \mathcal{G}_{BU}(\mathcal{P}) \cup \mathcal{G}_{UB}(\mathcal{P}) \cup \mathcal{G}_{UU}(\mathcal{P})$, where the subscripts B and U denote the bounded and unbounded components, respectively. The components are given by

$$\begin{aligned}
\mathcal{G}_{BB}(\mathcal{P}) &= \{(u, \mathcal{P}u) \mid u \in \mathcal{U} \cap L_\infty^{n_i}, \mathcal{P}u \in L_\infty^{n_o}\} \\
\mathcal{G}_{BU}(\mathcal{P}) &= \{(u, \mathcal{P}u) \mid u \in \mathcal{U} \cap L_\infty^{n_i}, \mathcal{P}u \in L_{\infty e}^{n_o} \setminus L_\infty^{n_o}\} \\
\mathcal{G}_{UB}(\mathcal{P}) &= \{(u, \mathcal{P}u) \mid u \in \mathcal{U} \cap L_{\infty e}^{n_i} \setminus L_\infty^{n_i}, \mathcal{P}u \in L_\infty^{n_o}\} \\
\mathcal{G}_{UU}(\mathcal{P}) &= \{(u, \mathcal{P}u) \mid u \in \mathcal{U} \cap L_{\infty e}^{n_i} \setminus L_\infty^{n_i}, \\
&\qquad \mathcal{P}u \in L_{\infty e}^{n_o} \setminus L_\infty^{n_o}\}.
\end{aligned}$$

In the bounded and unbounded partitioning of $\mathcal{G}(\mathcal{P})$, $\mathcal{G}_{BB}(\mathcal{P})$ denotes the desired i/o pairs, $\mathcal{G}_{BU}(\mathcal{P})$ describes the instabilites of the plant ("unstable poles") and $\mathcal{G}_{UB}(\mathcal{P})$ describes the instabilites in the inverse relation ("unstable seros"). Clearly, a feedback system stabilises $\mathcal{P}$ subject to bounded disturbances if and only if the closed-loop generates plant i/o pairs in $\mathcal{G}_{BB}(\mathcal{P})$. In other words, $\mathcal{G}_{BB}(\mathcal{P})$ must be nonempty. For example, for the particular map $\mathcal{P}$ from u to y where $\dot{y} = 1 + u^2$, has $\mathcal{G}_{BB}(\mathcal{P}) = \emptyset$, hence there cannot exist any stabilising scheme.

- Unless specifically emphasised, maps are not considered to be stable or algebraic.

Definition 2 (stable)
A causal map $\mathcal{H} : L_{\infty e}^{n_i} \rightarrow L_{\infty e}^{n_o}$ is said to be stable iff there exists a continuous nondecreasing $\phi_{\mathcal{H}} : \mathbb{R}_+ \rightarrow \mathbb{R}_+$ such that $\|\mathcal{H}u\| \leq \phi_{\mathcal{H}}(\|u\|)$ for all $u \in L_\infty^{n_i}$. $\diamond$

For a stable map $\mathcal{H}$, $\mathcal{G}_{BB}(\mathcal{H}) = L_\infty^{n_i} \times \mathcal{H}(L_\infty^{n_i})$; $\mathcal{G}_{BU}(\mathcal{H}) = \emptyset$; $\mathcal{G}_{UB}(\mathcal{H})$ may or may not be empty.

Definition 3 (unimodular)
A causal map $\mathcal{H} : L_{\infty e}^{n_i} \rightarrow L_{\infty e}^{n_i}$ is said to be unimodular iff $\mathcal{H}$ is stable, bijective and $\mathcal{H}^{-1}$ is stable. $\diamond$

For a unimodular map $\mathcal{H}$, $\mathcal{G}_{BB}(\mathcal{H}) = L_\infty^{n_i} \times L_\infty^{n_i}$; $\mathcal{G}_{BU}(\mathcal{H}) = \emptyset$; $\mathcal{G}_{UB}(\mathcal{H}) = \emptyset$; $\mathcal{G}_{UU}(\mathcal{H}) = (L_{\infty e}^{n_i} \setminus L_\infty^{n_i}) \times (L_{\infty e}^{n_i} \setminus L_\infty^{n_i})$.

Definition 4 (incrementally stable)
A causal map $\mathcal{H} : L_{\infty e}^{n_i} \rightarrow L_{\infty e}^{n_o}$ is said to be incrementally stable iff $\mathcal{H}$ is stable and there exists a continuous nondecreasing $\tilde{\phi}_{\mathcal{H}} : \mathbb{R}_+ \rightarrow \mathbb{R}_+$ such that for all $u \in L_{\infty e}^{n_i}$, $\|\mathcal{H}(u+v) - \mathcal{H}u\| \leq \tilde{\phi}_{\mathcal{H}}(\|v\|)$ for all $v \in L_\infty^{n_i}$. $\diamond$

For an incrementally stable map, bounded deviations in the input result in bounded deviations at the output. The bound on the output deviation is *independent* of the nominal input signal u.

In the case of an *algebraic* incrementally stable map $\mathcal{H}$ where the bounding function $\tilde{\phi}_{\mathcal{H}}$ is *linear*, the algebraic nonlinearity $\mathcal{H}$ is also referred to as Lipschitz continuous.

- From now on, the words bounded and stable will be interpreted in the sense of L_∞.
- The nonlinear unity-feedback system $S(\mathcal{P}, C)$ denotes the interconnection

$$\begin{aligned}
y &= \mathcal{P}u \\
u &= u_1 - C(u_2 + y) \quad ,
\end{aligned}$$

where u_1 and u_2 denote the exogenous inputs perturbing the actuator and sensor signals u and y, respectively (see Figure 1).

- The feedback system $S(\mathcal{P}, C)$ is said to be stable iff the map from (u_1, u_2) to (u, y) is stable.

Note that the stability of $S(\mathcal{P}, C)$ requires that the closed-loop map exists and it is stable. The well-posedness condition that ensures the existence of the map is almost always satisfied in practice, since $\mathcal{P}$ and/or C are strictly causal.

2 A Class of Feedback Linearizable Plants

Definition 5 ($\mathcal{L}$)
A causal nonlinear plant $\mathcal{P}$ is said to belong to the class $\mathcal{L}$ iff there exist a unimodular map $\mathcal{M}$, a linear

time-invariant map P with a finite-dimensional state-space representation, and a stable map $\mathcal{F}$ such that

$$\mathcal{P} = \mathcal{M}^{-1}P(I - \mathcal{F}\mathcal{M}^{-1}P)^{-1} \quad . \qquad (1)$$

In order to emphasize the particular triple $(\mathcal{M}, P, \mathcal{F})$ used, equation (1) will be denoted by $\mathcal{P} = \mathcal{L}(\mathcal{M}, P, \mathcal{F})$. $\diamond$

Note that if $\mathcal{P} = \mathcal{L}(\mathcal{M}, P, \mathcal{F})$ (see Figure 1) , the map from u to y can be expressed as

$$\mathcal{P} : u \mapsto y \begin{cases} \mathcal{M}y &= Pv \\ v &= u + \mathcal{F}y \end{cases} .$$

Applying the stable output-feedback

$$u = \vartheta - \mathcal{F}y$$

the map from ϑ to $\mathcal{M}y$ is rendered linear. Clearly, for a given $\mathcal{P} \in \mathcal{L}$, the triple $(\mathcal{M}, P, \mathcal{F})$ is not uniquely determined. The well-posedness of the feedback loop in the description of $\mathcal{P}$ is inherently assumed by the existence of the map from u to y ; in general, strict causality of P and/or $\mathcal{F}$ suffice for well-posedness of the feedback loop in $\mathcal{L}(\mathcal{M}, P, \mathcal{F})$.

This particular class of nonlinear plants in Definition 5 is in fact motivated by the special class of nonlinear plants that can be put in the controllable canonical form

$$\begin{aligned} \dot{x} &= f(x) + Bu \\ \zeta &= \Phi(x) \\ \dot{\zeta} &= A\zeta + B(u + F(x)) \quad , \end{aligned}$$

where Φ is an algebraic change of coordinates and F is an algebraic stable map. Note that for this particular case, $y = x$, $\mathcal{M}y = \Phi(y)$, $\mathcal{F}y = F(y)$ and $P = (sI - A)^{-1}B$.

For plants in $\mathcal{L}$, the linear part P admits coprime factorisations; let

$$P = ND^{-1} = \tilde{D}^{-1}\tilde{N} \qquad (2)$$

with the Bezout identity

$$\begin{bmatrix} \tilde{U} & \tilde{V} \\ -\tilde{D} & \tilde{N} \end{bmatrix} \begin{bmatrix} N & -V \\ D & U \end{bmatrix} = I \quad , \qquad (3)$$

where all of the eight maps are stable. By linearity, stable maps are also incrementally stable. Note also that for the description in (2) for a full rank P , the numerators drop rank at the zeros and the denominators drop rank at the poles. Since P is not necessarily single-input single-output, poles and zeros (except blocking zeros) may coincide. Since it is easier to describe the unstable zeros and unstable poles of P due to the transform algebra, one can easily describe the partitions $\mathcal{G}_{UB}(P)$ and $\mathcal{G}_{BU}(P)$. The following result establishes the connection between the graphs of P and $\mathcal{P} \in \mathcal{L}$.

Fact 6 (on graphs of P and $\mathcal{P}$)
If $\mathcal{P} = \mathcal{L}(\mathcal{M}, P, \mathcal{F})$, then there exists a unimodular map $\mathcal{T}$ such that

1. $\mathcal{G}_{BB}(\mathcal{P}) = \mathcal{T}\mathcal{G}_{BB}(P)$,
2. $\mathcal{G}_{UB}(\mathcal{P}) = \mathcal{T}\mathcal{G}_{UB}(P)$.

Proof: See Appendix. $\diamond$

Note that Fact 6 establishes that the desired i/o pairs and the unstable dynamics of the inverse relations are related in the graphs of P and $\mathcal{P}$. Such a simple description between the rest of graph partitions cannot be established in general.

We now consider the stabilization of plants in $\mathcal{L}$; i.e., determining a causal nonlinear map C such that the feedback system $S(\mathcal{P}, C)$ (see Figure 1) is stable.

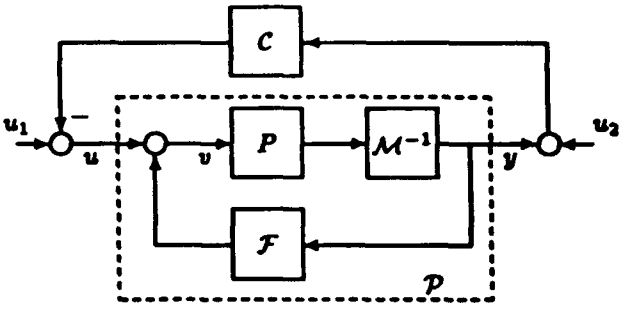

Figure 1: Feedback system $S(\mathcal{P}, C)$.

The existence of a transformation of $\mathcal{P}$ to a linear P , and Fact 6 suggests stabilization schemes based on designing controllers for P . The following conjectures emphasize this design approach.

Conjecture 7
For a given $\mathcal{P} = \mathcal{L}(\mathcal{M}, P, \mathcal{F})$, if $S(P, C_P)$ is stable then $S(\mathcal{P}, (C_P\mathcal{M} + \mathcal{F}))$ is stable. $\diamond$

Conjecture 7 is based on the design method of undoing the nonlinear maps $\mathcal{F}$ and $\mathcal{M}$, which consists of the following steps:
1. transform the nonlinear plant to an LTI one,
2. design a stabilising controller (possibly nonlinear) for the LTI plant and
3. using the inverse transformation and the designed controller for the LTI plant, determine the transformed controller for the nonlinear plant.

Conjecture 8
For a given $\mathcal{P} = \mathcal{L}(\mathcal{M}, P, \mathcal{F})$, if $S(\mathcal{P}, C)$ is stable then $S(P, (C - \mathcal{F})\mathcal{M}^{-1})$ is stable. $\diamond$

If Conjectures 7 and 8 were in fact true, one would end up with a necessary and sufficient condition for stabilising plants in $\mathcal{L}$ by merely using the transformations and nonlinear controller design methods based on linear plants. We now investigate these conjectures and state conditions (other than trivial cases like $\mathcal{P} = P = \mathcal{L}(I, P, 0)$) , under which related results can be established.

3 Stabilizing Feedback Linearizable Plants

The following fact (see e.g., [Kab1]) describes the set of all nonlinear stabilising compensators C_P in $S(P, C_P)$.

Fact 9 ($S(P)$)
Let the causal linear map P satisfy equations (2) and (3) . Under these assumptions, the feedback system $S(P, C_P)$ is stable if and only if $C_P \in S(P)$, where $S(P) = \{(U + DQ)(V - NQ)^{-1} \mid Q$ is stable and $(V - NQ)$is bijective with a causal inverse$\}$ $\diamond$

The following Lemma justifies the design approach in Conjecture 7 for a special subset of plants in $\mathcal{L}$.

Lemma 10 (A Sufficient Condition for Stabilising $\mathcal{L}(\mathcal{M}, P, \mathcal{F})$)
Let $\mathcal{P} = \mathcal{L}(\mathcal{M}, P, \mathcal{F})$, where the maps $\mathcal{F}$ and $\mathcal{M}$ are both incrementally stable. Under these assumptions, if $S(P, C_P)$ is stable then $S(\mathcal{P}, (C_P\mathcal{M} + \mathcal{F}))$ is stable.
Proof: See Appendix. ◇

The existence of a unimodular map that relates the desired input output pairs of P and $\mathcal{P}$ (see Fact 6-1) , is the main motivator for Conjectures 7 and 8 . The second part of Fact 6 relates the "unstable sero dynamics" of P and $\mathcal{P}$. For a precise description of the notion of sero dynamics in nonlinear systems that extend the well-known case in finite-dimensional linear time-invariant maps, see [Isi1] . Unlike the motivating controllable canonical form derivation, the class of nonlinear plants in $\mathcal{L}$ *can* have "unstable sero dynamics" . In fact, Lemma 10 does apply to such cases since one can easily stabilise P with unstable seros. The advantage of the class $\mathcal{L}$ is to take the stabilisation concept of algebraic-feedback linearisable systems under full-state feedback (which relies on constructing an output that has the sufficient relative degree to avoid "sero dynamics") to a larger class where the input output map already has "unstable sero dynamics" . The virtue of Fact 6-2 is that one does not need to determine the stability properties of the "sero dynamics" of the nonlinear map $\mathcal{P}$, which is a highly nontrivial task.

We now present a counterexample to Conjecture 7 .

Example 11
Consider the single state plant model $\mathcal{P}$ from u to y described by

$$\dot{y} = y^2 + u \quad .$$

Note that $\mathcal{P} = \mathcal{L}(I, 1/s, (\cdot)^2)$. Choose $C_P = I \in S(P)$. For $C = C_P\mathcal{M} + \mathcal{F} = I + (\cdot)^2$, the closedloop system $S(\mathcal{P}, C)$ is described by

$$\dot{y} = -(y + u_2) + y^2 - (y + u_2)^2 + u_1 \quad .$$

Clearly, for $u_2 = 0$, the closed-loop map from u_1 to (u, y) in $S(\mathcal{P}, C)$ is stable. However, for $u_2 \neq 0$, the closed-loop system $S(\mathcal{P}, C)$ is *not* stable. To see this, consider $u_1 = \delta_1$ and $u_2 = \delta_2$ where $\dot{\delta}_i = 0$, $i = 1, 2$. In other words, under constant sensor and actuator bias, the closed-loop system is described by

$$\dot{y} = -(1 + 2\delta_2)y + \delta_1 - \delta_2 - \delta_2^2 \quad .$$

Hence, for $\delta_2 \leq -0.5$, the output y is not bounded. ◇

Example 11 emphasizes the importance of checking the closed-loop map from (u_1, u_2) to (u, y) , rather than just u_1 to (u, y) . The same example also illustrates the effect of estimated state feedback and how the lack of a separation principle for nonlinear systems renders the design procedure heuristic, which happens to fail for this particular case. When an estimator with steady-state bounded bias is introduced in the ideal state-feedback, the closed-loop is no longer stable.

The problems with Conjectures 7 and 8 are mainly due to ignoring the exogenous input u_2 , and relying on the following fact.

Fact 12 (Conjectures 7 and 8 under no measurement noise)
For a given $\mathcal{P} = \mathcal{L}(\mathcal{M}, P, \mathcal{F})$, $S(P, C_P)\,|_{u_2=0}$ is stable if and only if $S(\mathcal{P}, C_P\mathcal{M} + \mathcal{F})\,|_{u_2=0}$ is stable. ◇

The instability mechanism in Example 11 can also be used to establish the lack of performance robustness under finite-energy disturbances, where u_1 and $u_2 \to 0$. Given any bound on the amplitude of y , there exists a finite-duration disturbance (hence finite-energy) such that the closed-loop output exceeds this bound before asymptotically reaching sero.

We now state the main result that shows the conservatism of basing the stabilisation of $\mathcal{P}$ on the stabilisation of P . The following theorem establishes that Conjecture 7 is not true in general and that incremental stability is of paramount importance.

Theorem 13 (Conservatism of Conjecture 7)
Let $\mathcal{P} = \mathcal{L}(\mathcal{M}, P, \mathcal{F})$ with $\mathcal{M}$ incrementally stable. Under these assumptions,
$S(\mathcal{P}, (C_P\mathcal{M} + \mathcal{F}))$ is stable for all $C_P \in S(P)$, if and only if $\mathcal{F}$ is incrementally stable.
Proof: See Appendix. ◇

Note that Theorem 13 emphasises that the design procedure is no longer decoupled (namely first stabilise P and then apply the transformed controller to $\mathcal{P}$) if the incremental stability of $\mathcal{F}$ fails. When incremental stability fails, Theorem 13 does not imply that there does not exist a compensator for P for which Conjecture 7 is valid. On the contrary, the selection of C_P is crucial as emphasised in the following example.

Example 14
Consider the plant $\mathcal{P}$ in Example 11 . Choose $C_P = I + (\cdot)^3$. Note that $C_P \in S(1/s)$ (see Appendix) . Apply the heuristic design procedure in Conjecture 7 , i.e., choose $C = C_P\mathcal{M} + \mathcal{F}$. The closed-loop system $S(\mathcal{P}, I + (\cdot)^2 + (\cdot)^3)$ is stable (see Appendix) . ◇

In order to show how restrictive it is to impose $\mathcal{M}$ and $\mathcal{F}$ are both incrementally stable, consider the following example.

Example 15
Consider the map $\mathcal{P}$ from u to y described by

$$\begin{aligned} \dot{x}_1 &= x_2 + f(x_1) \\ \dot{x}_2 &= x_3 \\ \dot{x}_3 &= u \\ x(0) &= 0 \\ y &= x \quad , \end{aligned}$$

where the algebraic nonlinearity f is bounded, i.e., there exists a $k > 0$ such that $|f(x)| \leq k$ for all $x \in \mathbb{R}$. Clearly, $f(\cdot)$, is stable and incrementally stable. Moreover, for any linear time-invariant finite-dimensional C such that $S(1/s^3[1 \;\; s \;\; s^2]^T, C)$ is stable, the interconnection $S(\mathcal{P}, C)$ is stable. Now consider the plant $\mathcal{P}$ in terms of the canonical form $\mathcal{L}$. Provided that f is at least twice differentiable, under the coordinate transformation

$$\mathcal{M} : x \mapsto \begin{bmatrix} x_1 \\ x_2 + f(x_1) \\ x_3 + x_2 f^{(1)}(x_1) + f(x_1) f^{(1)}(x_1) \end{bmatrix}$$

and algebraic feedback $\mathcal{F}x = x_2^2 f^{(2)}(x_1) + x_3 f^{(1)}(x_1) + 2x_2 f(x_1) f^{(2)}(x_1) + x_2 (f^{(1)}(x_1))^2 + f(x_1)(f^{(1)}(x_1))^2 + f^2(x_1) f^{(2)}(x_1)$, one has $\mathcal{P} = \mathcal{L}(\mathcal{M}, \frac{1}{s^3}\begin{bmatrix} 1 \\ s \\ s^2 \end{bmatrix}, \mathcal{F})$.

Clearly, $\mathcal{M}$ is unimodular and $\mathcal{F}$ is stable. However, unless $f^{(2)}$ vanishes, $\mathcal{F}$ is not incrementally stable. ◇

4 Conclusion

In the course of bounded-input bounded-ouput stabilisation of nonlinear plants, those that can be transformed into an LTI one are of particular interest due to a vast pool of theoretical and computational tools associated with LTI design problems. The existing transformation immediately suggests a simple design approach: design a stabilising control law for the transformed LTI plant and then use the transformed control law for the nonlinear plant. As it is shown in the study, such an approach is not a sure design procedure unless more restrictions are imposed on the transformation. The design for the transformed LTI plant is really not decoupled from the original nonlinear design problem; hence, one should not rule out intentionally nonlinear controller design for the transformed LTI plant. Although this might seemingly defy the purpose of the transformation, since the transformed design problem is yet another nonlinear control design problem, it also emphasises the need for more results in nonlinear control design for LTI plants. Along this line, for a given LTI plant, one has a complete parametrisation of all nonlinear stabilising controllers ; however, the choice of the parameter subject to a particular cost is not straightforward. Another approach is based on optimal control with non-quadratic integrand cost criteria from which nonlinear state-feedback laws are derived.

5 Appendix

Proof of Fact 6

Let $\mathcal{P} = \mathcal{L}(\mathcal{M}, P, \mathcal{F})$. From Figure 1, the equations relating the (u, y) pair and (v, Pv) pair define the map $\mathcal{T}$ as follows:

$$\begin{array}{rcll} \mathcal{T}(v, Pv) & = & (u, y) & = (v - \mathcal{F}\mathcal{M}^{-1}Pv, \mathcal{M}^{-1}Pv) \\ (v, Pv) & = & \mathcal{T}^{-1}(u, y) & = (u + \mathcal{F}y, \mathcal{M}y) \quad . \end{array}$$

Since $\mathcal{F}$ is stable and $\mathcal{M}$ is unimodular, $\mathcal{T}$ defined above is also unimodular. By unimodularity of $\mathcal{T}$,

$$(u, y) \in \mathcal{G}_{BB}(\mathcal{P}) \iff (v, Pv) \in \mathcal{G}_{BB}(P) \quad ,$$

which establishes Fact 6 1) .

Let $(u, y) \in \mathcal{G}_{UB}(\mathcal{P})$. Since $\mathcal{M}$ is stable, $Pv = \mathcal{M}y$ is bounded. Since u is unbounded and $\mathcal{F}\mathcal{M}^{-1}Pv$ is bounded, $v = u + \mathcal{F}\mathcal{M}^{-1}Pv$ is unbounded. Hence $(v, Pv) \in \mathcal{G}_{UB}(P)$. Similarly, v unbounded, Pv bounded imply y bounded and $u + \mathcal{F}y$ unbounded, hence u is unbounded. This establishes part 2) . □

Proof of Lemma 10

By Fact 9 , the stability of $S(P, C_P)$ implies that $C_P = (U + DQ)(V - NQ)^{-1}$, for some stable Q . Any input output pair corresponding to the map C_P can be expressed as the pair $((V - NQ)\xi, (U + DQ)\xi)$, where ξ denotes the pseudo-state of this particular factorization. For this particular factorization, the input output pair of C_P is bounded if and only if ξ is bounded. Moreover, since $\mathcal{F}$, $\mathcal{M}$ and $\mathcal{M}^{-1}$ are stable, the closed-loop system $S(\mathcal{P}, (C_P\mathcal{M} + \mathcal{F}))$ is stable if and only if the closed-loop map from (u_1, u_2) to ξ is stable. Writing the equations describing the feedback system $S(\mathcal{P}, (C_P\mathcal{M} + \mathcal{F}))$ in terms of ξ, we obtain (see Figure 1 and equation (2))

$$\tilde{D}\mathcal{M}y = \tilde{N}\left(u_1 + \mathcal{F}y - \mathcal{F}(u_2 + y) - (U + DQ)\xi \right) \quad (4)$$

$$(V - NQ)\xi = \mathcal{M}(u_2 + y) \quad . \quad (5)$$

Adding $\tilde{D}\mathcal{M}(u_2 + y)$ to both sides of (4), substituting (5) and (3) and using the linearity of $\tilde{N}$ and $\tilde{D}$, we obtain

$$\xi = \tilde{N}u_1 - \tilde{N}(\mathcal{F}(y + u_2) - \mathcal{F}y) + \tilde{D}(\mathcal{M}(y + u_2) - \mathcal{M}y) \quad .$$

Clearly, if $\mathcal{F}$ and $\mathcal{M}$ are incrementally stable, ξ is bounded for all bounded u_1 and u_2 . □

Proof of Theorem 1

"if" Follows by Lemma 10.

"only if" Follows by Example 11 , by setting $\mathcal{M} = I$, $P = 1/s$, $\mathcal{F} = (\cdot)^2$ and $C_P = 1$. □

Proof of the claim in Example 14

The closed loop system $S(1/s, I + (\cdot)^3)$ is described by

$$\dot{x} = u_1 - (x + u_2) - (x + u_2)^3 \quad .$$

The closed-loop system $S(\mathcal{P}, I + (\cdot)^2 + (\cdot)^3)$ is described by

$$\dot{x} = u_1 + x^2 - (x + u_2) - (x + u_2)^2 - (x + u_2)^3 \quad .$$

For u_1 and u_2 in L_∞ , using the Lyapunov function candidate $V(x) = x^2$, in both cases for $|x|$ sufficiently large $\dot{V}$ along the solution trajectories is eventually negative. Hence the closed-loop map from (u_1, u_2) to (u, x) is stable in both cases.

References

[Des1] C. A. Desoer and M. Vidyasagar, *Feedback Systems: Input-Output Properties*, Academic Press, 1975.

[Ham1] J. Hammer, "Fraction Representations of Non-Linear Systems: A Simplified Approach," *International Journal of Control*, vol. 46, no. 2, pp. 455–472, February 1987.

[Isi1] A. Isidori, *Nonlinear Control Systems* , Springer-Verlag, 1989.

[Kab1] M. G. Kabuli, *Factorization Approach to Nonlinear Feedback Systems* , Ph.D. Dissertation, University of California, Berkeley, 1989.

[Kan1] I. Kanellakopoulos, P. V. Kokotovic and A. S. Morse, "Systematic Design of Adaptive Controllers for Feedback Linearizable Systems," *IEEE Transactions on Automatic Control*, vol. 36, pp. 1241–1253, November 1991.

[Sas1] S. S. Sastry and A. Isidori, "Adaptive Control of Linearizable Systems," *IEEE Transactions on Automatic Control*, vol. 34, pp. 1123–1131, November 1989.

[Ver1] M. S. Verma, "Coprime Fractional Representations and Stability of Nonlinear Feedback Systems," *International Journal of Control*, vol. 48, pp. 897–918, 1988.

[Vid1] M. Vidyasagar and N. Viswanadham, "Stabilization of Linear and Nonlinear Dynamical Systems using an Observer-Controller Configuration," *Systems and Control Letters*, vol. 1, no. 2, pp. 87–91, 1981.

Appendix C

Appendix C includes a regular invited paper presented at the 1993 Automatic Control Conference.

"Real-Time Implementation Issues in Nonlinear Model Inversion,"
M. Güntekin Kabuli, Sudarshan P. Bhat and Robert L. Kosut,
Proceedings of the American Control Conference,
pp. 547–551, San Francisco, June 1993.

Proceedings of the
American Control Conference
San Francisco, California • June 1993

Real-Time Implementation Issues in Nonlinear Model Inversion

M. Güntekin Kabuli Sudarshan P. Bhat Robert L. Kosut *

Integrated Systems Inc., 3260 Jay Street, Santa Clara, CA 95054-3309

Abstract

A real-time control problem associated with a flexible testbed fixture is considered. The regulated variable is the deflection at the tip of a flexible beam attached to an inertia wheel base which is subject to a disturbance torque. The control torque affects the base wheel through a coupling which has both compliance and variable backlash. The performance specifications include disturbance attenuation and rapid slewing at the tip. The designs are based on an analytically derived continuous-time model which is tuned in accordance with the measured data. The model consists of an interconnection of a linear time-invariant part and piecewise-linear algebraic nonlinearities modeling friction and backlash. The candidate designs must be based on available measurements only; moreover, the final discrete-time control law must be executable with the real-time controller hardware limitations at hand.

Introduction

The first design approach is based on the linear model where the nonlinearities due to friction and backlash are set to zero. A single tone additive actuation disturbance is attenuated at the regulated output by incorporating the disturbance model in the feedback loop. Designs are based on a discretized plant model and implemented on an Integrated Systems AC-100 real-time control processor.

The second approach is a case study based on feedback linearization where a single parametric nonlinearity is included in the design model. Due to the nonminimum-phase zero dynamics characteristics from the actuation to the tip of the flexible beam, the study focuses on the base wheel position and slewing performance. We study the sensitivity of two certainty equivalence based control laws for the frozen parameter case. Based on the least sensitive non-adaptive design, an adaptive slewing controller is designed. This approach for slewing design is later modified to obtain a *baseline* design for attenuating a measured multitone disturbance. The disturbance model is based on a periodic torque waveform affecting the wheel base after the coupling driven by the actuator motor. The resulting continuous time control law was simulated to verify the performance enhancement due to the signal generator in the proposed feedforward/feedback scheme. One of the major tasks for real-time implementability was to obtain a discrete-time approximation to the continuous-time simulations of the nonlinear control law subject to the sampling rate and computational load limitations imposed by the real-time controller hardware. The approximate discretization was downloaded to the real-time controller processor and the continuous-time versus discrete-time simulation comparison proved to be satisfactory. The disturbance rejection part is a baseline design which is currently unimplementable unless the disturbance can be measured; however, the current discrete-time control law is an implementable candidate for real-time slewing tests.

Design Approach 1

An adaptive controller was designed for rejecting single tone sinusoidal disturbance in a prespecified frequency range. The controller consists of an inner-loop, robustly stabilizing component and an outer-loop, adaptive error rejection component. The control design was accomplished in three steps (see Figure 1) .

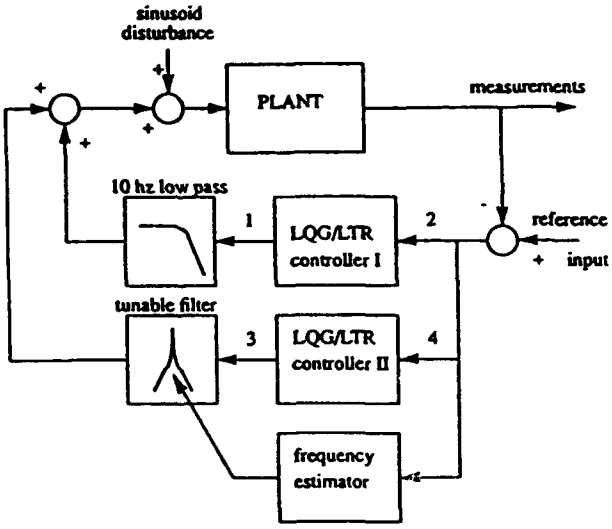

Figure 1:

The first step was the design of the inner loop controller. A 10 hz low pass filter was included in the loop to avoid any destabilizing loopgain in excess of 10 hz. This underscores the objective of actively controlling the rigid body slew mode and the first flexible mode (around 4.7 hz frequency range). This will also result in the flexible modes in excess of 10 hz to be unregulated. The stabilizing 'LQG/LTR controller I' in the innerloop was designed using the LQG/LTR design approach based on the input/output relation from '1' to '2' (see Figure 1) in the inner-loop in the absence of the outer loop; note that this requires an LQG/LTR design for an augmented plant which includes the actual plant cascaded by the 10 hz low pass filter at the input.

*Research supported by ARO, Engineering Sciences Division under contract DAAL03-91-C-0011 and AFOSR, Directorate of Aerospace Sciences under contract F49620-90-C-0064.

The second step was the design of the outer loop controller for rejection of a nominal single tone sinusoid disturbance frequency of 4 hz on plant. The outer error rejection loop contains a frequency shaping block that contains an undamped pole at 4 hz. This undamped pole provides an infinite gain at 4 hz which in a stabilizing loop assures perfect rejection of a single tone, 4 hz, sinusoid disturbance on the plant. A 20 dB attenuation on both directions from the 4 hz frequency assures the retaining of inner-loop characteristics outside the 4 hz range. The stabilizing 'LQG/LTR controller II' in the outerloop was designed using the LQG/LTR design approach, just like in the inner-loop, based on the input/output relation from '3' to '4' (see Figure 1) in the presence of the inner-loop. Figure 2 shows the LQG/LTR loop gain through the plant with the two stages of control (solid line) and with only the inner stage of control (dotted line). The corresponding sensitivities are shown in Figure 3 .

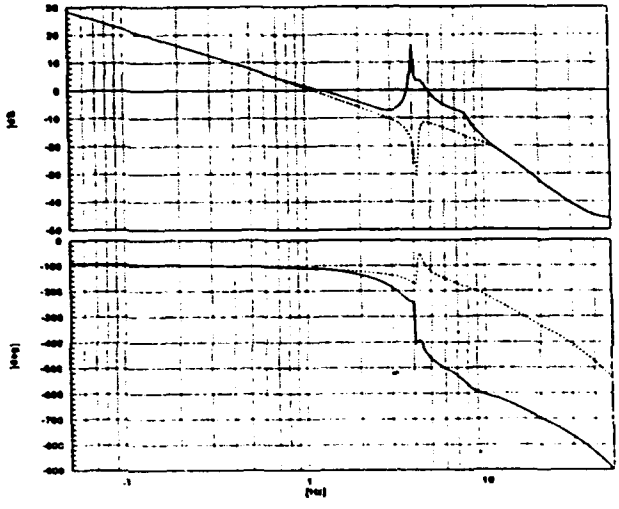

Figure 2:

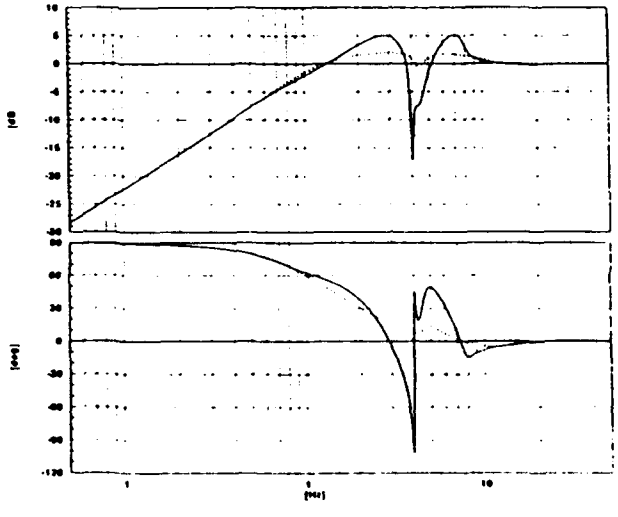

Figure 3:

The third step was the adaptive relocation of the undamped pole in the outer-loop shaping filter to the estimated frequency of disturbance. When the estimated frequency is equal to the actual frequency of a sinusoid disturbance and the resulting outer-loop is stable, a perfect disturbance rejection is guaranteed. The frequency of disturbance was estimated using an extended Kalman filter based on a notch filter. It is emphasized again that the only change from the two stage controller designed above is the adaptive tuning of the shaping filter in the outer loop. The entire inner loop and the 'LQG/LTR controller II' in the outer loop remain unchanged. Such an adaptive tuning was facilitated by the fact that the two stage loop was found analytically stable for the filter peak placed anywhere in the range 2 to 7 hz.

Figures 4 and 5 are plots generated from the data captured during a real-time implementation of the adaptive controller on the testbed fixture. A step response of the adaptive controller is shown in Figure 4 . The top seven strip charts plot the sensor measurement data from motor encoder, backlash encoder, iwheel encoder, strain gage 1, strain gage 2, motor velocity and tip accelerometer respectively. The bottom strip chart refers to the actuation voltage data to the motor. Figure 5 shows the same sensor measurements (top seven strip charts) for a steady 0.6 V sinusoid disturbance at the actuator with the disturbance frequency undergoing step changes (in hz) from from 4 to 3.75, 4 and 4.25 (8th strip). The 9th strip shows the real time estimate of the disturbance frequency. The strip data shows a disturbance buildup immediately following the step change in the disturbance frequency. This is followed by disturbance attenuation which occurs as the frequency of disturbance estimator locks on to the true frequency of the sinusoid disturbance. Adaptation and complete disturbance rejection is accomplished within 5 to 10 seconds following a step change in the disturbance frequency.

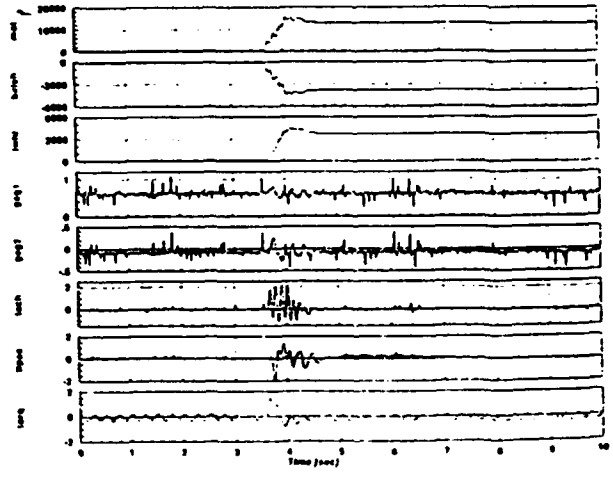

Figure 4:

The adaptive controller presented here was not able to handle disturbance rejection on the testbed fixture in the range 4.6 to 4.8 hz (also confirmed from analytical simulations). This behavior can be attributed to the presence of a lightly damped flexible mode around 4.7 hz. The adaptation mechanism could lock on the disturbance frequency only if the sensor measurements were dominated by the single tone of the disturbance. With the disturbance frequency in the 4.6 to 4.8 hz range, the sensor measurements also contained a significant contribution from the lightly damped mode.

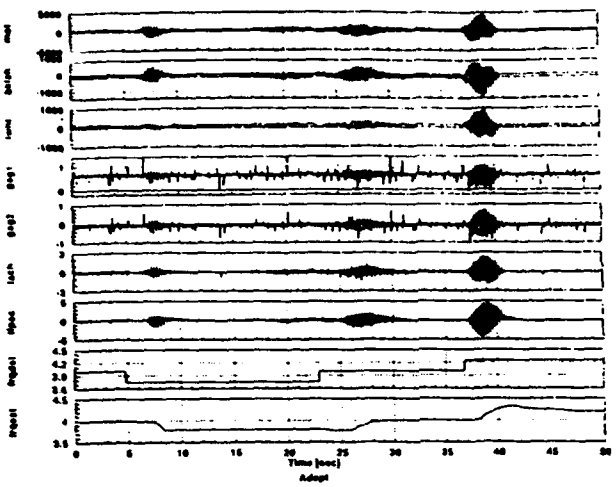

Figure 5:

This situation resulted in the frequency estimator flip-flop-ing between the two dominant frequencies, resulting in ringing.

Design Approach 2

Consider the nonlinear plant model shown in Figure 6 , where G denotes the *known* linear part and $\mathcal{F}$ denotes the algebraic nonlinearity (e.g., friction, saturation) which depends on an *unknown* parameter θ . The signals v_i and v_o at the input and output of the nonlinearity are *unavailable* as measurements. The disturbances and regulated variables are denoted by w and z , respectively. The goal is to determine a control input u such that using only the measurement at y, the output y asymptotically tracks a desired reference signal.

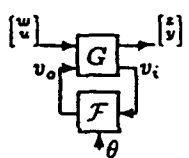

Figure 6:

The adaptive scheme we are investigating is based on a feedforward-feedback configuration (see Figure 7). This configuration gives rise to two nontrivial subproblems: 1) Sensitivity of the non-adaptive design, i.e., the stability and tracking robustness of the closed-loop subject to perturbations of $\hat{\theta}$ about the nominal θ and 2) Parameter estimation. Without closing the loop via the parameter estimator in Figure 7, we first design a tracking controller based on a known signal $\hat{\theta}$. The motivation behind the sensitivity study is that for sufficiently slow adaptation, one recovers the performance of the inherent tracking design. Hence, the goal is to determine the least-sensitive non-adaptive design. So far, our studies have shown that among other tracking designs based on the certainty-equivalence principle (use the parameter estimate *as if* it were correct), the underlying design in Figure 7 is consistently the least sensitive. For a known parameter estimate $\hat{\theta}$, a candidate input-output pair $(\hat{u}, \hat{y})$ is generated using the model in Figure 6 with θ replaced by $\hat{\theta}$. The tracking controller C_T achieves the desired tracking of the reference signal r in the loop with the model $\hat{\mathcal{P}}$. This input-output pair $(\hat{u}, \hat{y})$ is injected to a feedback system where C_R stabilizes the actual plant; C_R alone need not be a tracking compensator. This approach improves the "performance bandwidth" without increasing the "control bandwidth" of the feedback system. Hence it has the potential of improving existing controller performance without a total redesign.

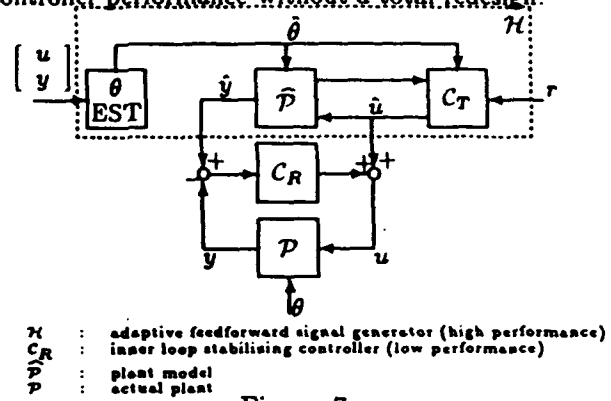

Figure 7:

The plant model is of the form

$$\begin{aligned} \dot{x} &= Ax + b_u u + b_w(w - \theta f(\dot{y})) \\ y &= c_y x \end{aligned}$$

where the 10 state, relative degree 3 SISO system (c_y, A, b_u) is minimum-phase with a lightly damped zero at 3.25 Hz . The algebraic nonlinearity $f(\cdot) = \text{sat}_1(40\cdot)$, where sat_1 is the odd symmetric piecewise-linear saturation function with unity slope and ± 1 saturation limits. In the rest of this study $\hat{f}(\cdot) = \tanh(40\cdot)$ will denote the smooth approximation to f . The periodic disturbance torque is denoted by w . Using $y, \dot{y}, y^{(2)}$, the control u determined by

$$\begin{aligned} \beta_2 u = u_l - \alpha_2 x - \beta_3(w - \theta f(\dot{y})) \\ +\beta_1(\dot{\theta} f(\dot{y}) + \theta f^{(1)}(\dot{y}) y^{(2)} - \dot{w}) \ , \end{aligned}$$

for appropriate coefficients α and β , renders $y^{(3)} = u_l$. Let $\mathcal{L}$ denote the associated map (i.e., from x, w, $\dot{w}$, θ, f to u_l) . Note that $\mathcal{L}$ can only be realized in the ideal case where x, w, $\dot{w}$, θ and f are all known. Although such is not the case, it still is interesting to note that the steady-state actuation demand to decouple y from w is given by $\frac{1}{\beta_2}(\beta_3 w + \beta_1 \dot{w})$. For the particular periodic w and actuation limits at hand, this translates into disturbance rejection of up to 7 harmonics of w . Similarly let $\hat{\mathcal{L}}$ denote the map depending on the available signals $\hat{x}$, $\hat{w}$, $\dot{\hat{w}}$, $\hat{\theta}$ and the smooth approximation $\hat{f}$.

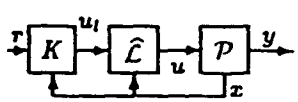

Figure 8:

Sensitivity of the nominal design

Consider the interconnection in Figure 8 , and a 10 mrad slew with the desired tracking performance for $\hat{\mathcal{L}} = \mathcal{L}$ as shown in Figure 9 (lower curves) . The solid and dashed lines denote the base and tip positions, respectively. The periodic disturbances w and $\dot{w}$ are exactly canceled. Note that the feedback linearization results in the inversion which causes the lightly damped 3.25 Hz mode. In the upper curves the mismatch is *only* f vs $\hat{f}$; i.e, x, w, $\dot{w}$, θ are exactly used in the feedback linearizer except that the algebraic nonlinearities are not identical. Performance degradation is self-explanatory.

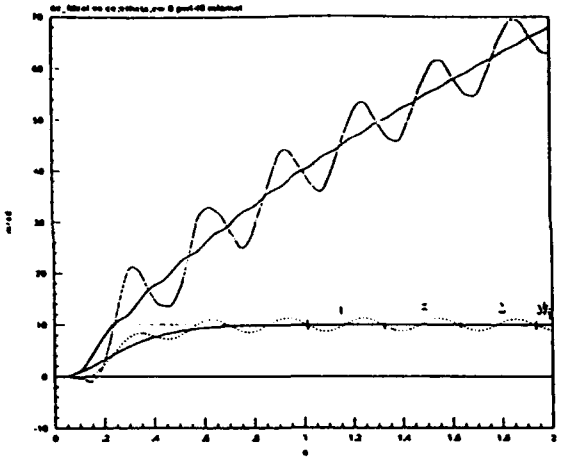

Figure 9:

Due to the sensitivity of the one-loop implementation of the certainty-equivalence principle in Figure 8 , we resorted to the certainty-equivalence based control scheme as shown in Figure 10 (redrawn from Figure 7 for ease of comparison with Figure 8) . A simple controller $C = 10$ stabilized the inner loop. The performance, on the other hand, depends on the generated signals $(\hat{u}, \hat{y})$. Our design studies have shown that the model-follower scheme in Figure 10 consistently proves to be the least sensitive to mismatches. These observations are mainly due to the fact that the inner-loop is inherently stable and the performance depends on the *cascade* structure. However, in Figure 8 , *both* stability and tracking performance have to be achieved in one loop.

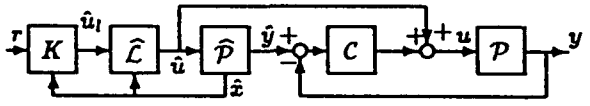

Figure 10:

Adaptive Slewing with $w = 0$

A parameter estimation block is introduced in the certainty-equivalence based tracking control design scheme in Figure 10 , to complete the interconnection as shown in Figure 7 . The disturbance w and the initial conditions $x(0) = \hat{x}(0)$ are assumed to be zero ; however, $\theta \neq \hat{\theta}$ and $f \neq \hat{f}$. Moreover, the state x is not being used in the control law and the parameter estimator solely depends on available signals u and y . In other words, for the disturbance free case, the interconnections in Figure 10 and Figure 7 are candidates for *implementable* designs since they depend on available signals only. However, real-time implementation requires the extra step of control law discretization, which proves to be a nontrivial task as it will be emphasized later on.

Consider Figure 11 . The dashed line denotes the the signal generator output trajectory (i.e., $\hat{y}$) and the solid line denotes the basewheel yaw (i.e., y) . The reference signal r is a smooth ± 20 mrad periodic waveform which $\hat{y}$ tracks after 4 seconds. Note that the output y tracks r within 1 mrad after approximately 6 seconds. There are two important points to be made about these responses: 1) the signal generator depends on $\hat{\theta}$ which is not constant (depends on the parameter estimator output waveform). Moreover, unlike the case in Figure 10 , when the parameter estimator loop is closed, $\hat{\theta}$ is no longer an exogenous signal for the signal generator, hence for slow adaptation (over the 6 second window), $\hat{y}$ also exhibits transient response (see dashed lines over the first 4 seconds in Figure 11) . When $\hat{\theta}$ is an exogenous signal, the signal generator is designed so that $\hat{y}$ tracks r in less than a second. 2) due to f and $\hat{f}$ mismatch, even with $\theta = \hat{\theta}$, the ideal tracking performance in the lower solid line in Figure 8 degrades to 1 mrad off at 2 seconds ; hence the offset emphasized by parallel lines in Figure 11 . The parameter estimator output (i.e., $\hat{\theta}$) is shown in Figure 12 .

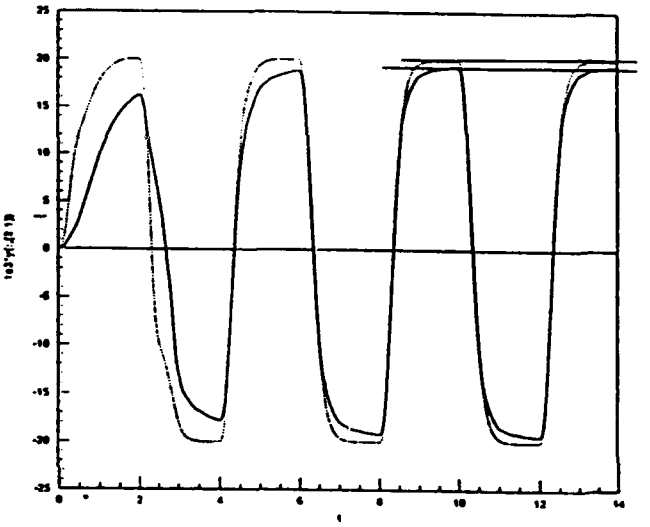

Figure 11:

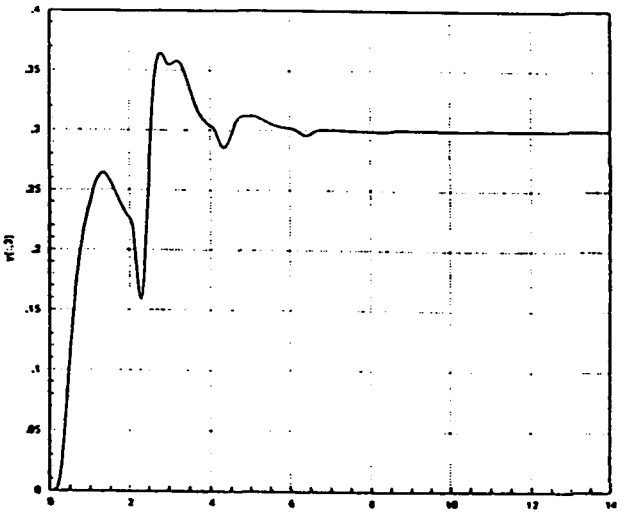

Figure 12:

Baseline disturbance rejection design and discretization issues

In order to illustrate the approach, consider the case where the interconnection in Figure 10 is LTI and modified to incorporate the disturbance w ; the disturbance

estimate used in the signal generator will be denoted by $\hat{w}$. The LTI plant from (w, u) to y is denoted by $[P_{yw}\ ,\ P_{yu}]$ and C denotes an LTI stabilizing compensator. Let

$$\begin{aligned} y &= P_{yu}(\hat{u} + C(\hat{y} - y)) + P_{yw}w \\ \hat{y} &= P_{yu}\hat{u} + P_{yw}\hat{w} \quad , \end{aligned}$$

where $\hat{y}$ denotes the desired plant output. Let e_y and e_w denote the errors $(y - \hat{y})$ and $(w - \hat{w})$, respectively. Then

$$e_y = (I + P_{yu}C)^{-1}P_{yw}e_w \quad .$$

Clearly, there are two options: 1) relying on the poles of $P_{yu}C$ at the disturbance poles or 2) choosing C to be any stabilizing controller and trying to set $e_w \rightarrow 0$. In the following baseline design, we will make the assumption that the disturbance w is periodic with a known period and can be *measured* . Even with these stringent assumptions, deriving a *discrete-time* implementation of the feedback linearization based model-follower scheme turned out to be a nontrivial task. In fact, even if w is assumed to be measured, the disturbance does not come in additive at the plant input; canceling the effect of w at y requires higher order derivatives of w . Since the performance depends on the success of cancellation, the derivatives are not constructed by filtered/delayed versions of w ; instead, an identifier is built to determine the Fourier coefficients of the harmonics of interest and the signal generator outputs $(\hat{u}, \hat{y})$ are derived accordingly. Throughout this process, the inner-loop controller is chosen as a simple gain $C = 10$; the inner-loop is inherently stable, and the w identifier generates the $\hat{w}$ information used in the signal generator. Throughout the following, there is a nonlinearity mismatch ; the plant model in the inner-loop uses f , whereas the signal generator uses the smooth version $\hat{f}$. The parameters satisfy $\theta = \hat{\theta} = 0.3$. A continuous-time design was completed ; the next step was to recover the continuous-time simulation results using a discrete-time controller. A maximum sampling rate of 400 Hz is dictated by hardware limitations. The minimum step-size of 2.5 ms was not small enough to reasonable replicate the nonlinear ordinary differential equation solution with *any* fixed step-size integration algorithm. The final successful discretization was based on the 4th order Runge-Kutta algorithm, which requires intersample point evaluation. In order to avoid oversampling, the controller was decomposed into an LTI system in feedback with algebraic nonlinearities and the LTI subsystem was discretized using the 4th order Runge-Kutta algorithm, introducing additional states as many as the inputs, to avoid intersampling. Using this particular discretization at 400 Hz, the continuous-time performance was sufficiently reproduced (see Figures 13 and 14) .

The two strip plots in Figure 13 correspond to the tip position before and after the model-follower is included ; the base is commanded a -3 mrad slew. The top strip is the tip position for the inner-loop controller $C = 10$, $\hat{u} = 0$, $\hat{y} = -3$ mrad (see Figure 10) . The disturbance w is periodic. The lower strip corresponds to the case where $\hat{w}$ is identified up to the first 7 harmonics and the $\hat{w}$ information is used in the signal generator to command the basewheel a -3 mrad slew and to cancel the effect of the 7 harmonics . Initially, the identifier coefficients are all zero ; it takes approximately 1 second for the parameters to converge. After

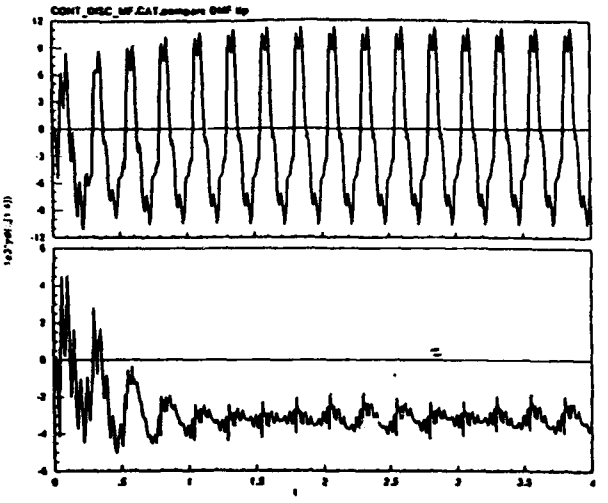

Figure 13:

1 second, the base is at -3 mrad and the tip has approximately ±1 mrad deviation (see lower strip, Figure 13) .

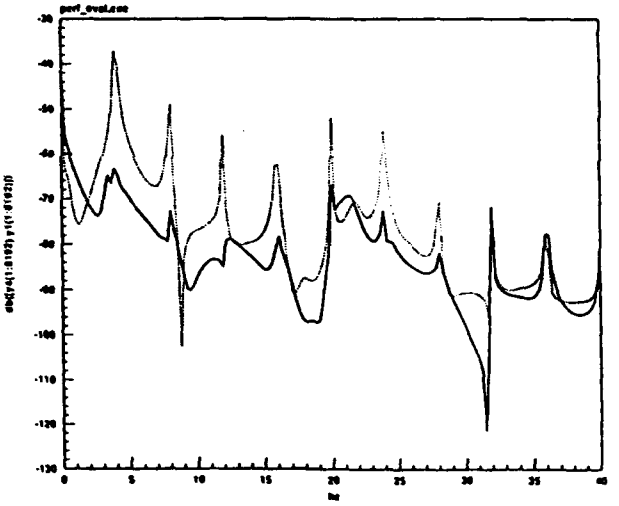

Figure 14:

Since the performance plots in Figure 13 do not correspond to an LTI system, one cannot represent the reduction of the harmonic term contributions directly. Although a transfer function description does not exist, we can still compare the frequency contents of each signal to substantiate the reduction of the harmonics at the tip. Using the discrete Fourier transforms of the two signals in Figure 13 , we obtain Figure 14 . The dashed and solid lines, respectively denote before and after the model-follower is introduced. The disturbance is 4 Hz periodic, and the identifier was built for the first seven harmonics. Hence the improvements are apparent up to 28 Hz , with reductions 26, 26, 26, 16, 16, 16 and 10 dB at 4, 8, 12, 16, 20, 24 and 28 Hz, respectively.